

University of Windsor

Scholarship at UWindor

Electronic Theses and Dissertations

Theses, Dissertations, and Major Papers

3-10-2019

Exploring the roles of the CXXC motifs in Cystathionine γ -Lyase

Scott Smith

University of Windsor

Follow this and additional works at: <https://scholar.uwindsor.ca/etd>

Recommended Citation

Smith, Scott, "Exploring the roles of the CXXC motifs in Cystathionine γ -Lyase" (2019). *Electronic Theses and Dissertations*. 7658.

<https://scholar.uwindsor.ca/etd/7658>

This online database contains the full-text of PhD dissertations and Masters' theses of University of Windsor students from 1954 forward. These documents are made available for personal study and research purposes only, in accordance with the Canadian Copyright Act and the Creative Commons license—CC BY-NC-ND (Attribution, Non-Commercial, No Derivative Works). Under this license, works must always be attributed to the copyright holder (original author), cannot be used for any commercial purposes, and may not be altered. Any other use would require the permission of the copyright holder. Students may inquire about withdrawing their dissertation and/or thesis from this database. For additional inquiries, please contact the repository administrator via email (scholarship@uwindsor.ca) or by telephone at 519-253-3000ext. 3208.

Exploring the roles of the CXXC motifs in Cystathionine γ -Lyase

By

Scott Andrew Smith

A Thesis

Submitted to the Faculty of Graduate Studies
through the Department of Chemistry and Biochemistry
in Partial Fulfillment of the Requirements for
the Degree of Master of Science
at the University of Windsor

Windsor, Ontario, Canada

2019

© 2019 Scott Andrew Smith

Exploring the Roles of the CxxC Motifs in Cystathionine γ -Lyase

by

Scott Andrew Smith

APPROVED BY:

J. Hudson
Department of Biological Sciences

J. Gauld
Department of Chemistry & Biochemistry

B. Mutus, Advisor
Department of Chemistry & Biochemistry

January 16, 2019

DECLARATION OF ORIGINALITY

I hereby certify that I am the sole author of this thesis and that no part of this thesis has been published or submitted for publication.

I certify that, to the best of my knowledge, my thesis does not infringe upon anyone's copyright nor violate any proprietary rights and that any ideas, techniques, quotations, or any other material from the work of other people included in my thesis, published or otherwise, are fully acknowledged in accordance with the standard referencing practices. Furthermore, to the extent that I have included copyrighted material that surpasses the bounds of fair dealing within the meaning of the Canada Copyright Act, I certify that I have obtained a written permission from the copyright owner(s) to include such material(s) in my thesis and have included copies of such copyright clearances to my appendix.

I declare that this is a true copy of my thesis, including any final revisions, as approved by my thesis committee and the Graduate Studies office, and that this thesis has not been submitted for a higher degree to any other University or Institution.

ABSTRACT

Hydrogen sulfide was known as a toxic, flammable gas, until 1996 when it was shown that H₂S plays an active role within the body. Cystathionine γ -lyase (CSE) is one of the enzymes responsible for the production of H₂S within the body. Little to nothing is understood about the regulation of CSE, specifically two conserved CxxC residues found in each monomer of the enzyme. The work aimed to identify the possible regulatory or catalytic role of each CxxC motif within CSE. Site-directed mutagenesis revealed the effect of each cysteine residue on the catabolism of cystathionine, as well as its effect on varying pH. The Cys252 residue was shown to be of genetic importance; point mutation of this residue rendered the enzyme inactive. Cys255, Cys307, and Cys310 showed little to no impact on the function of the enzyme. Cys₃₀₇-X-X-Cys₃₁₀ is located on the periphery of the enzyme, while Cys₂₅₂-X-X-Cys₂₅₅ is located in the interior, at the dimer-dimer interface. This suggests a structural role for the 200 CxxC and a more catalytic role for the 300 motif.

The catalytic potential of the 300 motif was interrogated with synthesized free thiol fluorescent probes, which mimic an already established one in the Mutus lab. The Cys₃₀₇-X-X-Cys₃₁₀ motif exhibited a specificity toward the FITC₂-homocystine probe, due to the nature of the dihedral disulfide bond angle. This was further shown through fluorescent kinetics, as well as a fluorescent labeling and imaging system based around SDS-PAGE. Lastly, mass spectrometry was employed to detect the modification site, but no positive result has been observed thus far. However, holoenzyme mass spectrometry has shown an addition of homocystine to the Cys307 and Cys310, as well as the *WT* enzyme. Together, this provides a strong indication of a secondary active site responsible for the reduction of homocystine to feed downstream pathways which CSE is implicated in.

DEDICATION

To my parents, and Kayla

ACKNOWLEDGEMENTS

I would first like to acknowledge and thank my supervisor, Dr. Bulent Mutus for his wonderful guidance and support that he has shown to me throughout my graduate studies. He provided me with the opportunity to complete my degree in a welcome and supportive environment, and for that I am forever grateful.

I also extend my thanks to my committee members, Dr.'s James Gauld and John Hudson. This research project would not have been completed without their meaningful insight and critical evaluation of my thesis.

For the smooth operation of the Department of Chemistry and Biochemistry, I give thanks to Beth Kickham, Marlene Bezaire, Catherine Wilson, and Joe Lichaa, the department could not be what it is without their tireless work and support. I would also extend my thanks to all other support staff and the CCC for all that they do.

A special thanks needs to be extended to Mutus lab members, both past and present; without you all I wouldn't have been able to finish my work. Thanks to Cody Caba for first showing me the ropes of the Mutus lab, and to Katie Fontana, my fellow rookie graduate student. I would like to thank both of my former undergraduate students, Mitchell Dipasquale and Leslie Ventimiglia, for all that they did for me and for the project. To all other members, Dave, for his wonderful coffee, Nemaka and Angela, thank you all for your company. I would also like to extend a special thanks to Justin Roberto, who was always available to help me with whatever problem I had. To all other graduate students, I thank you all for the wonderful memories and friendships.

To Dr. Janeen Auld, I extend a special thanks for her help in the running and

analysis of my many mass spectrometry samples that I brought forth. As well as to Dr. Otis Vacratsis, you provided valuable insight when consulted with the many problems with my mass spectrometry data.

TABLE OF CONTENTS

DECLARATION OF ORIGINALITY	iii
ABSTRACT	iv
DEDICATION	v
ACKNOWLEDGEMENTS	vi
LIST OF TABLES	x
LIST OF FIGURES	xi
LIST OF APPENDICES	xiii
LIST OF ABBREVIATIONS & NOMENCLATURE	xiv
CHAPTER 1: INTRODUCTION	1
1.1 <i>Hydrogen Sulfide</i>	2
1.1.1 <i>Biological Properties of Hydrogen Sulfide</i>	2
1.1.2 <i>Hydrogen Sulfide as a Gasotransmitter</i>	3
1.1.2 <i>Postulated Physiological Roles of Hydrogen Sulfide</i>	4
1.1.2.1 <i>Reactive Oxygen Species-Scavenger</i>	4
1.1.2.2 <i>Biological Impact of Hydrogen Sulfide on Cardiovascular, Neurological, and Inflammatory Response</i>	7
1.1.3 <i>Postulated Hydrogen Sulfide Signaling Pathways</i>	11
1.1.4 <i>Measurement of Hydrogen Sulfide</i>	12
1.2 <i>In vivo Hydrogen Sulfide Production</i>	17
1.2.1 <i>Reverse Transsulfuration Pathway</i>	17
1.2.2 <i>Cysteine Catabolism</i>	22
1.2.3 <i>Cystathionine γ-lyase</i>	22
1.3 <i>CxxC Motif</i>	25
1.4 <i>Fluorogenic Free Thiol Probes</i>	27
1.5 <i>Research Objective and Rationale</i>	29
CHAPTER 2: MATERIALS AND METHODS	30

2.1	<i>Materials and Chemicals</i>	31
2.2	<i>Methods</i>	33
2.2.1	<i>Site Directed Mutagenesis</i>	33
2.2.2	<i>Plasmid Miniprep</i>	34
2.2.3	<i>Bacterial Plasmid Transformation</i>	34
2.2.4	<i>Purification of CSE</i>	35
2.2.5	<i>In Vitro Kinetic Assays</i>	36
2.2.6	<i>Probe Synthesis and Purification</i>	40
2.2.7	<i>Fluorescent Labelling of CSE</i>	41
2.2.8	<i>Mass Spectrometry</i>	43
2.2.9	<i>Molecular Modelling</i>	46
2.2.10	<i>Statistical Analysis</i>	46
CHAPTER 3: RESULTS		47
3.1	<i>Site Directed Mutagenesis</i>	48
3.2	<i>In-vitro Kinetic Assays</i>	48
3.3	<i>pH Dependent Activity of CSE Mutants</i>	53
3.4	<i>Di-E-GSSG as a CSE Pseudo Substrate</i>	55
3.5	<i>Novel Fluorescent Free Thiol Probes</i>	55
3.6	<i>Mass Spectrometry</i>	63
CHAPTER 4: DISCUSSION.....		68
4.1	<i>CSE In-vitro Kinetics</i>	69
4.2	<i>Fluorescent Free Thiol Probes</i>	71
4.3	<i>Mass Spectrometry</i>	73
CHAPTER 5: CONCLUSION		76
REFERENCES/BIBLIOGRAPHY.....		78
APPENDICES		85
	Appendix A (<i>Chapters 1 & 2 supplementary material</i>).....	85
	Appendix B (<i>Chapters 3 & 4 supplementary material</i>).....	89
VITA AUCTORIS		95

LIST OF TABLES

1.1	Reported maximum sensitivity, as well as common reported ranges for blood and tissue H ₂ S concentrations for common H ₂ S measurement techniques.	14
3.1	Extracted kinetic parameters of all CSE constructs.	51

LIST OF FIGURES

1.1	Visual representation of the 3 effects of H ₂ S on oxidative stress	6
1.2	H ₂ S effects on Alzheimer's and Huntington's	10
1.3	Canonical Reverse Transsulfuration Pathway	18
1.4	CBS catalyzed reactions	19
1.5	CSE catalyzed reactions	20
1.6	Crystal structure of CSE and active site	23
1.7	CxxC disulfide redox mechanism	25
1.8	Synthesis of an FITC based probe	27
3.1	CSE catabolism of L-cystathionine by <i>WT</i> and mutants	50
3.2	pH dependent activity curves for <i>WT</i> and all functionally active mutants	53
3.3	Fluorescent fold increase after DTT incubation and proposed structures of FITC-based probes	56
3.4	Fluorescent free thiol kinetics	57
3.5	Visualization and quantification of free thiol probe-based labelling	60
3.6	Mass Spectrometry fingerprint for Cys ₂₅₂ -X-X-Cys ₂₅₅ and Cys ₃₀₇ -X-X-Cys ₃₁₀ motifs	62-63

LIST OF APPENDICES

Tables

A.1	Table of PCR primers used for site-directed mutagenesis	86
------------	---------------------------------------------------------	----

Figures

A.1	CSE plasmid map	84
A.2	hCSE sequence with emphasis on CxxC motifs	85
A.3	Purification and purity check of <i>WT</i> and mutant CSE enzymes	87
B.1	Effects of post-translational modifications on CSE	88
B.2	Di-E-GSSG CSE kinetics	89
B.3	Space filling model of CSE (2NMP), MM2 energy minimized probe structures	90
B.4	<i>WT</i> mass spectrometry chromatogram	91
B.5	TLHVRMEK, identifying peptide for CSE	92
B.6	LLEAAITPETK, identifying peptide for CSE	93

LIST OF ABBREVIATIONS & NOMENCLATURE

2 x YT	Yeast Extract Tryptone
3- MST	3-mercaptopyruvate sulfurtransferase
Apo E	Apolipoprotein E
ARE	Antioxidant Responsive Element
ATF4	Activating Transcription Factor 4
Aβ	Amyloid Beta
BACE-1	Beta-site Amyloid Precursor Protein Cleaving Enzyme-1
cAMP	Cyclic Adenosine Monophosphate
CBS	Cystathionine β -synthase
CO	Carbon Monoxide
CSE	Cystathionine γ -lyase
Cys	Cysteine
di-E-GSSG	Di-Eosin-Glutathione disulfide
DTT	Dithiothreitol
EAAT2	Excitatory Amino Acid Transporters-2
FITC	Fluorescein Isothiocyanate
FSQ	Fluorescence Self-quenching
GC	Gas Chromatography
GCL	γ -glutamylcysteine synthetase
GSH	Glutathione
GSSH	Glutathione Persulfide
H₂S	Hydrogen Sulfide
HCN	Hydrogen Cyanide
HD	Huntington's

HS⁻	Hydrosulfide
ICAM-1	Intracellular Adhesion Molecule-1
Keap1	Kelch-like ECH Associated Protein 1
LMW	Low Molecular Weight
MBB	Monobromobimane
mhtt	Mutant Huntington Protein
NFκB	Nuclear Factor Kappa-light-chain-enhancer of Activated B
NMDA	N-methyl-D-aspartate
NO	Nitric Oxide
Nrf2	Nuclear Factor (erythroid-derived 2)-like 2
PAG	Propargylglycine
PERK	Protein Kinase-like Endoplasmic Reticulum Kinase
PKA	Protein Kinase A
PKCε-STAT-3	Protein Kinase C Epsilon-Signal transducer and Activator of transcription 3
PKG	Protein Kinase G
PLP	Pyridoxal-5`-phosphate
PLP	Pyridoxal-5`-Phosphate
PTP-1B	Tyrosine Phosphatase-1B
ROS	Reactive Oxygen Species
RSS⁻	Persulfide
RSS_nSR	Polysulfide
S²⁻	Sulfide
S₂O₃²⁻	Thiosulfate
SO₄²⁻	Sulfate
VEGF-Akt-eNOS-NO-cGMP	Vascular Endothelial Growth Factor Protein Kinase

B- Nitric Oxide Synthase 3-Nitric Oxide-cyclic
Guanosine Monophosphate

CHAPTER 1:
INTRODUCTION

1.1 Hydrogen Sulfide

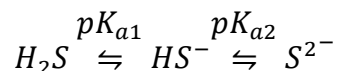
Hydrogen Sulfide (H_2S) was first discovered in 1777 by Carl William Scheele, a Swedish-German pharmaceutical chemist responsible for the isolation of oxygen and hydrogen among others [1, 2]. Produced from the decomposition of organic matter, H_2S is commonly found in natural gas, and volcanic emissions. It is associated with heavy-industries such as oil and gas production, asphalt production and cooling, paper mills and sewage treatment [3-6]. Incidentally, indirect exposure to H_2S pollution has been shown to cause an increase in the rate of spontaneous abortions [7].

1.1.1 Biological Properties of Hydrogen Sulfide

Hydrogen Sulfide is a colourless, flammable, gas with a characteristically repugnant odour, like that of rotten eggs. Short term exposure to high concentrations of H_2S can lead to lethal sulfide poisoning which shares a similar mechanism of effect to that of cyanide. In both hydrogen cyanide (HCN) and H_2S poisoning, HCN and H_2S are tightly bound to the binuclear center of cytochrome c oxidase, specifically the oxidized heme a_3 decreasing cellular respiration [8-10]. Cytochrome c Oxidase is responsible for the transfer of electrons from ferrocytochrome c to molecular oxygen, which is then converted to water during oxidative phosphorylation [11].

Hydrogen sulfide exists in the body in 3 main states: (i) free sulfide, which is defined as dissolved H_2S , exists as an equilibrium between H_2S , HS^- and S^{2-} , (ii) acid-labile sulfur which is sulfur released under acidic conditions from iron-sulfur complexes common in enzymes, (iii) bound sulfane sulfur, or covalently bound sulfur, commonly found in persulfides, polysulfides, and Na_2S [12-14]. Hydrogen sulfide is a weak diprotic acid

which can further dissociate to both hydrosulfide (HS^-), and sulfide (S^{2-}), as shown in **Equation 1.1**. Under physiologically relevant conditions $\text{p}K_{a1}$ occurs at 6.76 while differing $\text{p}K_{a2}$ values have been reported, ranging from 17-19 [15, 16]. With $\text{p}K_{a2} > 17$, the amount of S^{2-} found within the body is negligible. The remainder of free sulfide found in cells is a nearly equal ratio of $\text{H}_2\text{S}/\text{HS}^-$, while in extracellular fluid and plasma there exists a 20% $\text{H}_2\text{S}/80\%$ ratio under relevant conditions [14].



Equation 1.1

Hydrosulfide is unable to diffuse across lipid membranes and tends to accumulate at its source. Once protonated, H_2S is lipophilic, and can freely diffuse through membranes [14, 17]. The lipophilic properties of H_2S in conjunction with the large variance in the cellular compartmentalization of H_2S , make the determination of H_2S concentration in the body a complex issue.

1.1.2 Hydrogen Sulfide as a Gasotransmitter

Carbon monoxide (CO) and nitric oxide (NO) are physiologically relevant gaseous molecules capable of initiating and eliciting a cellular signaling response; as such they have been classified as gasotransmitters. Wang described gasotransmitters using 6 criteria: (i) the molecules must be gaseous, (ii) they do not require transporters to diffuse through membranes, (iii) they are endogenously generated *via* enzymatic activity and their generation is regulated, (iv) at physiologically relevant concentrations and pH they have defined roles, (v) possess specific molecular targets, (vi) functions displayed by the gas can be mimicked by exogenous addition of said gas [18, 19]. Hydrogen sulfides effect on both

the enhancement of N-methyl-D-aspartate (NMDA) receptor-mediated responses as well as the induction of long-term potentiation in the hippocampus, as shown by Abe and Kimura, was some of the first evidence that H₂S played a vital role in signaling [20]. H₂S's involvement in neuromodulation, smooth muscle relaxation, and K_{ATP} channels among others, led Wang to propose H₂S as a gasotransmitter [19, 21].

1.1.2 Postulated Physiological Roles of Hydrogen Sulfide

1.1.2.1 Reactive Oxygen Species-Scavenger

Hydrogen sulfide combats oxidative stress by scavenging free radicals and reactive oxygen species (ROS). Hydrogen sulfide can be oxidized to sulfate (SO₄²⁻), thiosulfate (S₂O₃²⁻), persulfides (RSS⁻), and polysulfides (RSS_nSR) among others. Oxygen and H₂S do not readily react, so relatively strong oxidants are required to oxidize H₂S. Hydrogen sulfide is a suitable scavenger of hydroxyls, carbonate radicals, and nitrogen dioxide, among others [22]. However, hydrogen sulfides potential as a scavenger of free radicals and ROS is wholly dependent on free H₂S concentration which can be as low as 10-30 nM in the brain [23]. However, H₂S can exhibit antioxidant effects by interacting with other enzymes and pathways. Glutathione (GSH) is a known antioxidant and scavenger of ROS such as glutamate. Glutamate is known to cause oxidative stress through a process called oxidative glutamate toxicity, or oxytosis [24]. Hydrogen sulfide has been shown to increase glutathione levels to combat oxytosis through several channels, shown in **Figure 1.1**. First, activity of γ -glutamylcysteine synthetase (GCL) is upregulated, which increases GSH synthesis. Second, H₂S promotes glutamate uptake into the cell by increasing the trafficking of the excitatory amino acid transporters-2 (EAAT2). Increased levels of intracellular glutamate also increase the rate of cystine transport into the cell through the

system x_c^- cystine/glutamate antiporter. Cystine, as well as its reduced form of cysteine are required by γ -glutamylcysteine synthetase for glutathione synthesis. Lastly, H_2S can reduce extracellular cystine to cysteine, increasing intracellular cysteine levels. Increased levels of intracellular cysteine show a greater effect on GSH synthesis than that of transported cystine [24-27].

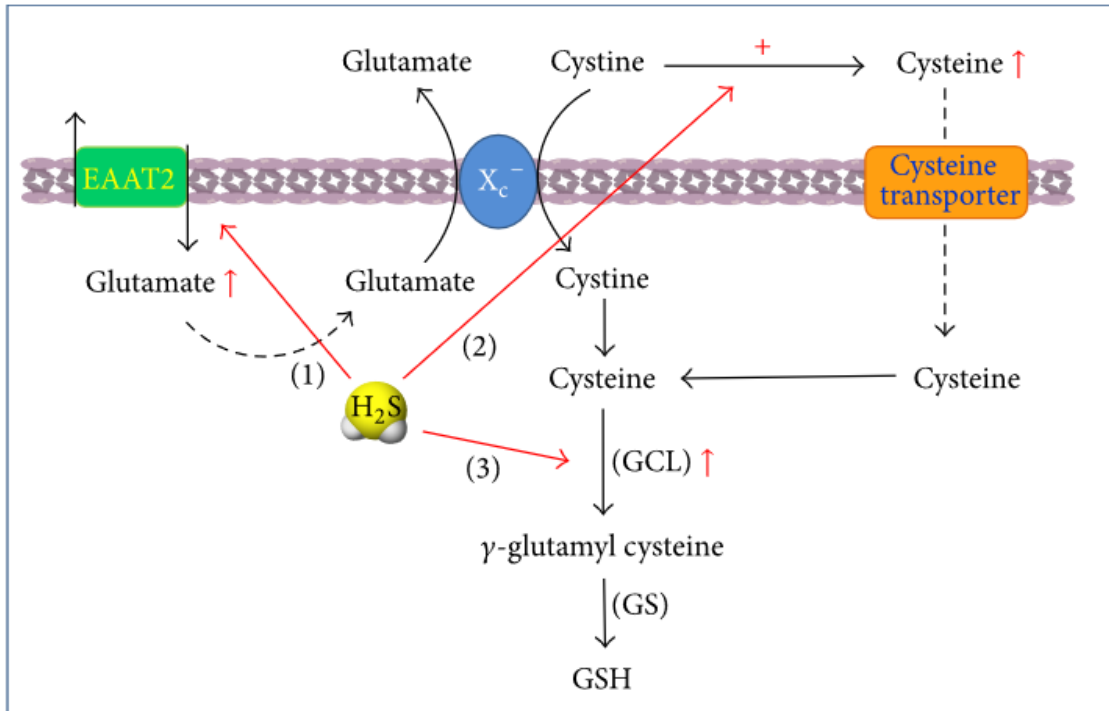


Figure 1.1 Visual representation of the 3 effects of H₂S on oxidative stress. 1) H₂S directly upregulates GCL increasing GSH levels. 2) Hydrogen sulfide increases trafficking of EAAT2, leading to increased cystine transport. 3) Reduction of cystine to cysteine increases intracellular cysteine, increasing GSH synthesis. (adapted from [28]).

1.1.2.2 Biological Impact of Hydrogen Sulfide on Cardiovascular, Neurological, and Inflammatory Response

Hydrogen sulfide has been shown to influence a myriad of major biological systems within the body, many of which can be attributed to its role in redox biology. Cystathionine γ -lyase (CSE) is responsible for the majority of H₂S production in the cardiovascular system as it is predominantly expressed within the cardiovascular system, specifically vascular endothelial cells, smooth muscle cells, and cardiomyocytes [21, 29-34]. In the cardiovascular system, H₂S has been shown to play a role in slowing myocardial ischemia reperfusion injuries, the promotion of angiogenesis, relaxation of smooth muscle cells (vasodilation), and, as stated earlier, in the regulation of blood pressure [21, 29, 31, 34, 35]. Patients with chronic heart disease or heart failure have had their levels of circulating H₂S shown to be significantly reduced when compared to an age-matched control [36]. Furthermore, it was demonstrated in CSE knockout mice that at the time of a cardiac event, administration of H₂S reduced infarct size by 72%, while overexpression of CSE severely limits the effect of injury [31]. Antiatherosclerotic properties have also been associated with H₂S. Loss of CSE expression, as seen in Apolipoprotein E (Apo E) mice treated with propargylglycine, a CSE inhibitor, is linked to the rapid development of atherosclerotic lesions and plaques. Treated mice showed decreased aortic H₂S production and plasma levels while conversely showing increased plasma levels of intracellular adhesion molecule-1 (ICAM-1), a biomarker for the buildup of atherosclerotic plaque in blood vessels [37-39].

The cardioprotective effects of H₂S are the result of several interactions with various signaling pathways. For example, H₂S induces nuclear localization of nuclear

factor (erythroid-derived 2)-like 2 (Nrf2), a transcription factor known for the regulation of gene expression of several anti-oxidant enzymes. This results in Nrf2 binding to the antioxidant responsive element (ARE), which is responsible for an increase in expression of hem oxygenase-1 (HO-1) and Thioredoxin-1 (Trx1), which are involved in stress response [40, 41]. Additionally, H₂S activation of the PKC ϵ -STAT-3 pro-survival signaling cascade directly contributes to an increase in cardioprotection. Additionally, this causes phosphorylation and inhibition of Bad, a pro-apoptotic factor, responsible for the death of cardiomyocytes [31, 39, 40]. Hydrogen sulfide often exhibits crosstalk with NO to elicit cardioprotective effects. For instance, addition of exogenous H₂S activates a VEGF-Akt-eNOS-NO-cGMP pathway which leads to a significant increase in NO concentrations, ultimately leading to a decrease in oxidative stress, while preserving mitochondrial function [36].

Like the cardiovascular system, H₂S has numerous effects upon the nervous system. As previously stated, H₂S affects hippocampal long-term potentiation by acting upon NMDA receptors [20]. Specifically, H₂S increases intercellular levels of cyclic adenosine monophosphate (cAMP) levels which increase activity of protein kinase A (PKA), leading to activation of NMDA receptors *via* PKA phosphorylation [42]. Various ion channels have been identified as potential targets of H₂S, as seen already through the effects of H₂S on K_{ATP} channels involved in vasodilation/constriction [29]. Calcium ion channels are a potential target of H₂S, shown by an increase in intracellular Ca²⁺ levels, as well as subsequent Ca²⁺ waves [43]. Likewise, modulation of both the Na⁺/H⁺ and Cl⁻/HCO₃⁻ exchangers by H₂S leads to intracellular acidification [44].

Effects of H₂S can also be seen in neurodegenerative diseases, specifically

Alzheimer's and Huntington's (HD), as can be seen in **Figure 1.2**. Both diseases show either a significant decline in H₂S levels or a significant lack of production when compared to healthy individuals [45, 46]. In Alzheimer's disease, treatment of rat models with exogenous H₂S inhibited expression of beta-site amyloid precursor protein cleaving enzyme-1 (BACE-1), a β -secretase involved in the production of amyloid beta (A β). Formation of the A β particles themselves can be inhibited by H₂S through the inhibition of γ -secretase activity *via* a cAMP dependent pathway after treatment with an exogenous H₂S donor [47, 48],

A defect in the activating transcription factor 4 (ATF4), a protein responsible for the disposition of amino acids stems from oxidative stress caused by cysteine. A lack of H₂S production caused by low levels of CSE, as well as low levels of key cysteine/cystine transporters EAAT3 and system x_c⁻ (as seen in **Figure 1.1**) increases levels of oxidative stress [49]. As well, the HD mutant protein mhtt sequesters SP1, the transcription factor for CSE, creating a feedback loop where no CSE can be produced, leading to massive increases of oxidative stress [49].

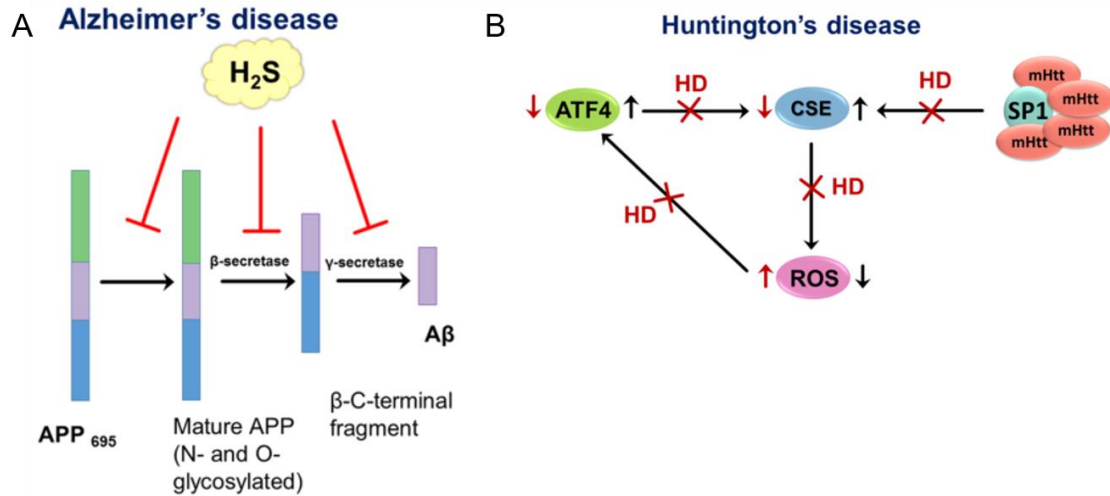


Figure 1.2. (A) Hydrogen sulfide's effect on Alzheimer's disease, displaying the inhibitory effect of both β-secretase and γ-secretase. (B) Huntington's disease schematic indicating the increase in reactive oxygen species due to lack of CSE expression due to mhtt, as well as decrease in ATF4 expression due to ROS. Modified from [50].

A case can be made that H₂S shows both pro and anti-inflammatory properties [51]. Hydrogen sulfide has shown proinflammatory effects on pancreatitis, as well as in ischemia reperfusion injury models of the kidney. Incidences of sepsis and septic shock have shown a proinflammatory effect associated to H₂S, as patients in sepsis have higher levels of H₂S [51, 52]. Anti-inflammatory properties of hydrogen sulfide have been touched upon lightly thus far, specifically in the cardiovascular effects section. Decrease in expression of ICAM-1 by exogenous H₂S treatment, and inhibition of NF-κB activity decrease inflammation [38, 53].

The effects of H₂S within the body are not limited to inflammation and the cardiovascular and nervous systems. Hydrogen sulfide plays prominent roles in the respiratory, reproductive, and renal system, while effecting the liver and gut [54-60]. Effects can be observed in hibernation and oxygen sensing, while a small, albeit somewhat controversial role, can be said for cancer [61, 62].

1.1.3 Postulated Hydrogen Sulfide Signaling Pathways

The biological mechanism of action that H₂S utilizes to elicit signaling events is most accepted to be through posttranslational modification of proteins. Hydrogen sulfide directly modifies cysteine residues with the help of an oxidant, as seen in **Equation 1.2**. This process is termed s-sulfuration, or, as it is more commonly known now, persulfidation.



Equation 1.2

Reactive persulfides in the form of RSS⁻/RSSH can form *via* H₂S interacting with cysteine residues on protein, however, H₂S displays low reactivity with oxidized thiols like those found in disulfides [63]. The requirement for an oxidant to post translationally modify a

protein *via* H₂S seems evolutionarily disadvantageous, however, two enzymes of the transsulfuration pathway, CSE and its counterpart, cystathionine β-synthase (CBS) catalyze reactions that result in the formation of several low molecular weight (LMW) persulfides [64]. In addition to Cys-SSH produced by CSE and CBS, glutathione persulfide (GSSH) can form through a persulfide exchange reaction in solution between Cys-SSH and GSH [65, 66].

Some Direct evidence of persulfide-based signaling have been observed. As previously stated, Hosoki et al showed that H₂S acts as a smooth muscle relaxant. It was later shown that H₂S's observed effects on K_{ATP} channels were a result of persulfidation of a cysteine residue located in a K_{ATP} channel subunit, Kir6.1. Persulfidation of this residue prevents ATP from interacting with the ion channel, resulting in a K⁺ influx and smooth muscle relaxation [29, 67]. Persulfidation of cysteine 215 in protein tyrosine phosphatase-1B (PTP-1B) results in a loss of enzymatic activity and an increase in phosphorylation. This increased phosphorylation increases the activation of protein kinase-like endoplasmic reticulum kinase (PERK) in response to ER stress [68].

Nuclear localization of Nrf-2, as mentioned previously, is partially responsible for the cardioprotective elements attributed to H₂S. Binding of Nrf-2 to ARE is a required step in the response to cardiac injury, however Nrf-2 is sequestered in the cytoplasm when inactive by Kelch-like ECH associated protein 1 (Keap1) [69, 70]. While the exact mechanism is not known, some form of oxidative or electrophilic modification of critical cysteine residues on Keap1 is required to induce a conformational change and facilitate the release of Nrf-2, resulting in transport to the nucleus [69, 70].

1.1.4 Measurement of Hydrogen Sulfide

The most significant issue in the field of H₂S biology is the accurate measurement of H₂S concentration within the body. There exist several methods for the measurement of endogenous H₂S as well as labile-sulfur species, such as methylene blue, sulfide ion specific electrodes (ISE), ion chromatography (IC), sulfide sensitive fluorescent dyes (SSFD), Monobromobimane (MBB), and gas chromatography, coupled to both mass spectrometry and flame photometric detectors (FPD). Issues arise when techniques designed for measurement of H₂S in the environment are erroneously applied to the body. The vast array of methods available to measure H₂S, and their vastly different sensitivities result in reported concentration ranges from the low nM to high μM range as seen in **Table 1.1**.

Table 1.1. Reported maximum sensitivity, as well as common reported ranges for blood and tissue H₂S concentrations for common H₂S measurement techniques.

<i>Method</i>	<i>Sensitivity</i>	<i>Blood (μM)</i>	<i>Tissue (μM)</i>
Methylene blue	>1 μM	20–300	40–200
Sulfide ISE	>1 μM	20–300	20–300
GC-FPD, IC	low nM	nd	nd
MBB	low nM	0.1–1	
Headspace, CG Polarographic (amperometric)	low nM 0.2 μM	0.01 nd–<1	low nM nd–<1
SSFD	>1 μM		

The methylene blue assay is the most commonly used colorimetric detection method. It involves the reaction of H₂S with *N,N*-dimethyl-*p*-phenylenediamine sulfate resulting in the product methylene blue which can be read at 670nm. Methylene blue was originally intended to measure H₂S concentration in air [71, 72]. Methylene blue also requires a highly acidic sample prep which has the potential to liberate acid-labile sulfur, further inflating reported concentrations. In addition to over-inflating H₂S concentrations, methylene blue can form dimers and trimers in solution, resulting in absorption values that do not follow Beer's Law [73]. The methylene blue assay routinely returns blood H₂S concentration values in the range of 20-300 μM; at such high concentrations, humans can experience eye and lung irritation, to unconsciousness and death within 4-8 hours [74]. Monobromobimane reacts quickly with H₂S, and under basic conditions to form a fluorescent product that can be separated by HPLC coupled to a fluorescent detector. The MBB reaction has a sensitivity of 2nM, while generally reporting plasma H₂S concentrations in the 0.1-1.0 μM range [75, 76]. At the low end H₂S is detectable by a human nose, while at the extreme plasma would have an offensive odour [74].

Polarographic electrodes and gas chromatography are two of the most accurate methods of H₂S measurement. Polarographic electrodes are very similar to standard oxygen sensors. The detection limit is in the range of 10-20 nM H₂S, and the H₂S specific membrane allows for real-time measurement of plasma or tissue samples in real time [75, 77]. Gas chromatography (GC) is often coupled to a flame photometric detector or mass spectrometer. Gas chromatography often reports values similar to those of the electrode, in the low nanomolar range [75]. While GC often measures both H₂S and acid-labile sulfur, it is possible to distinguish between the two if pH is carefully controlled [78].

When examining the literature, one must consider any reported H₂S concentrations, as well as the method used to determine that value. It is also critical to examine the claims attributed to H₂S made in older literature and evaluate whether the method used to measure concentrations is both accurate and trustworthy.

1.2 In vivo Hydrogen Sulfide Production

1.2.1 Reverse Transsulfuration Pathway

Hydrogen sulfide is produced mainly in the cardiovascular system, liver, kidneys and the brain. It is a common byproduct of the metabolic pathway known as the transsulfuration pathway. The transsulfuration pathway involves the interconversion of cysteine and homocysteine through a cystathionine intermediate catalyzed by the successive actions of two pyridoxal-phosphate containing enzymes, cystathionine β -synthase and cystathionine γ -lyase [79, 80]. These two enzymes are predominantly located in the cytosol, with some reports indicating they are found in the nucleus and mitochondrion [81-83]. There are two versions of this metabolic pathway, the forward and reverse. The forward transsulfuration pathway involves the conversion of cysteine to homocysteine *via* the actions of CSE and CBS, and ultimately the methylation of homocysteine to methionine *via* methionine synthase [84]. The canonical reverse transsulfuration pathway, **Figure 1.3**, involves the interconversion of homocysteine and serine to cystathionine through the function of CBS, followed by the beta elimination of the C- γ -S bond of cystathionine to yield cysteine [85]. While the reverse transsulfuration pathway is responsible for cysteine production, which is used in glutathione biosynthesis, both enzymes are capable of producing both H₂S and LMW persulfides [64]. This is a result of both enzymes showing levels of substrate promiscuity with other sulfur containing

species. All auxiliary CBS catalyzed reactions can be seen in **Figure 1.4**, while **Figure 1.5** displays reactions catalyzed by CSE.

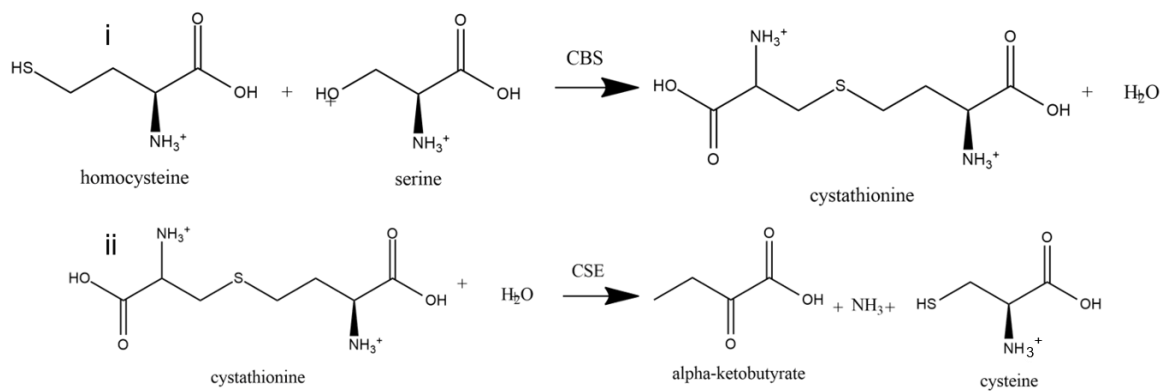


Figure 1.3 Canonical reverse transsulfuration pathway. (i) Dehydration of homocysteine and serine to form cystathionine, catalyzed by CBS. (ii) CSE catalyzed hydrolysis of cystathionine to alpha-ketobutyrate, ammonia, and cysteine.

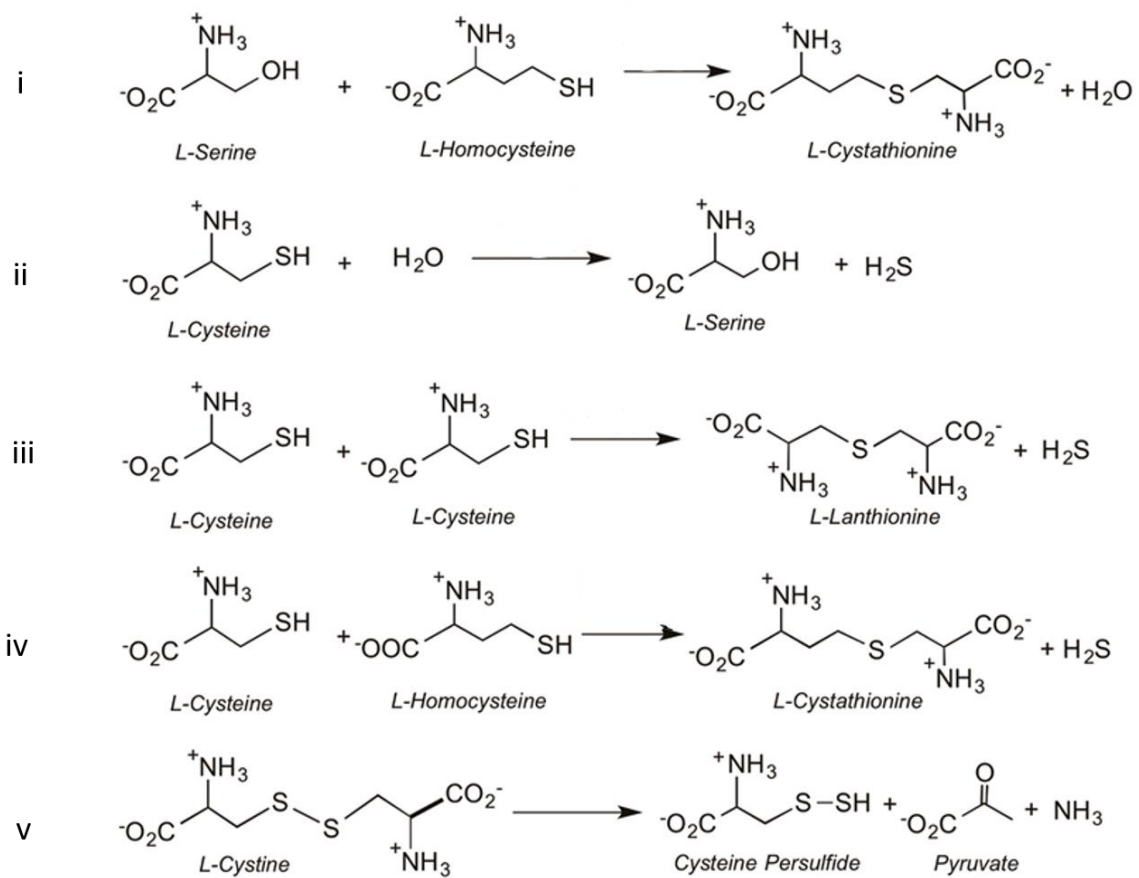


Figure 1.4 Reactions catalyzed by CBS. Reactions ii, iii, and iv are responsible for H₂S production, while reaction v is responsible for the production of cysteine persulfides.

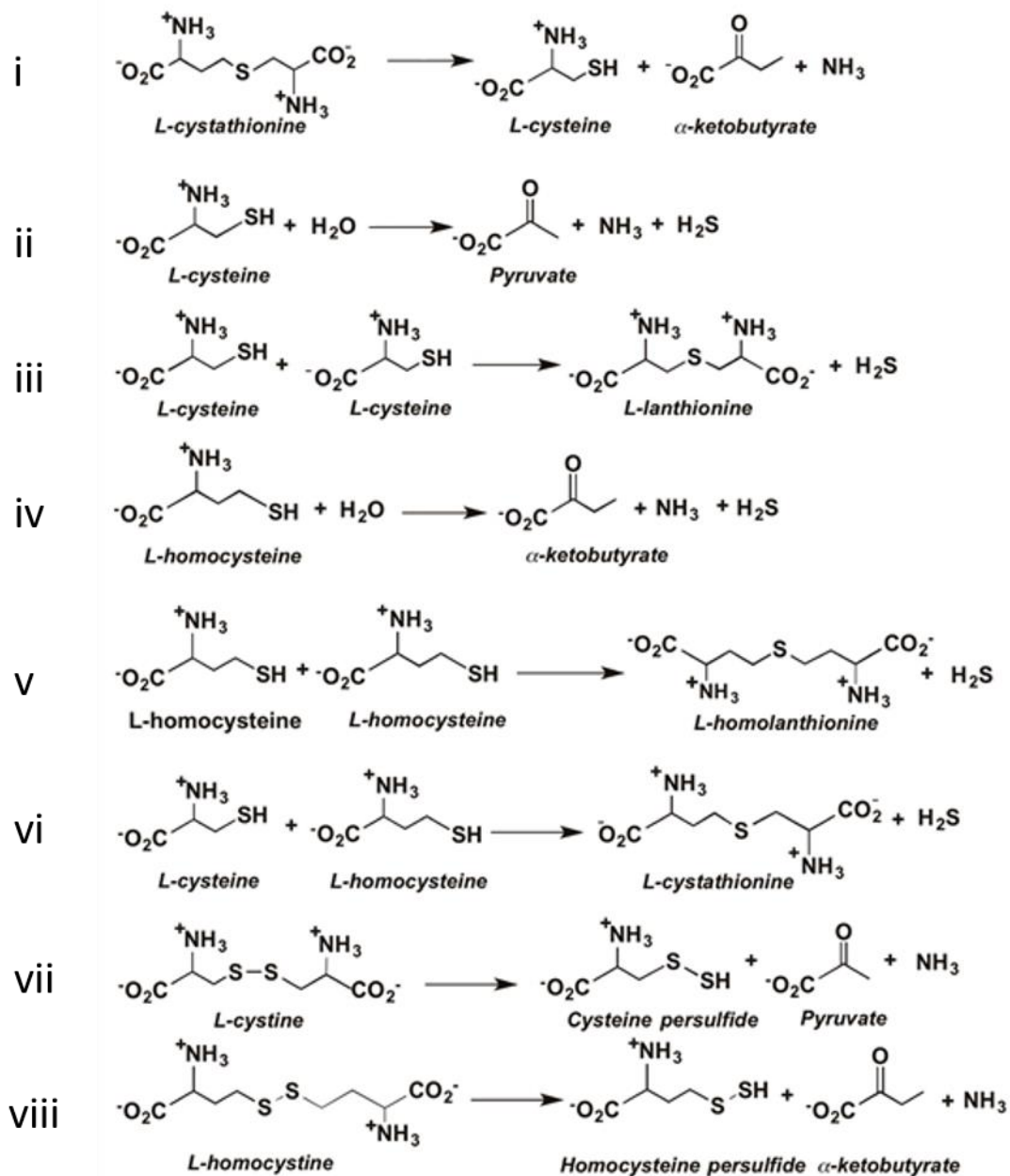


Figure 1.5 Reactions catalyzed by CSE. Reactions ii-vi are responsible for the production of H₂S. Reactions vii and viii are the cysteine and homocysteine persulfide producing reactions. The preferred substrate, cysteine, can be seen in reaction ii.

1.2.2 Cysteine Catabolism

In addition to production of H₂S through the transsulfuration pathway, the enzyme 3-mercaptopyruvate sulfurtransferase (3-MST) catalyzes the transfer of sulfur from cysteine to that of a small, nucleophilic thiol acceptor. Hydrogen sulfide is then liberated from the sulfide acceptor [86].

1.2.3 Cystathionine γ -lyase

Cystathionine γ -lyase (EC 4.4.1.1), the second enzyme of the transsulfuration pathway, is a PLP-dependent beta-replacing lyase which is located on chromosome 1, p31.1, in humans. There are two separate isoforms of CSE, one of which is the result of a 132 base pair deletion. While both isoforms are expressed, the longer form is the dominant form [87]. CSE is predominantly expressed in the cardiovascular system and respiratory system, as evidenced by its large cardioprotective effects [21, 29]. In addition, CSE is the main H₂S forming enzyme in the kidneys, liver, uterus and placenta [21, 88].

Cystathionine γ -lyase is a 44.5 kDa monomer which associates as a homotetramer in solution, shown in **Figure 1.6**. Interestingly, crystal structures have shown PLP binding in only three of the four subunits. Pyridoxal-phosphate interacts with CSE through strong hydrogen bonding between the phosphate and two subunits, specifically Gly90, Leu91, Ser209, Thr211 from the primary PLP binding subunit, and Tyr60 and Arg62 from an adjacent subunit. Supplemental to these hydrogen bonds are two key bonds between Asp187 and Lys212 with PLP. A Schiff base is formed between the carbonyl carbon of PLP and amino group of Lys212, while Asp187 is involved electrostatically with the pyridinium ring. Additionally, Tyr114 and the pyridine ring of PLP exhibit aromatic π -stacking [89]. Cystathionine γ -lyase inhibition is possible by propargylglycine (PAG), β -

cyanoalanine, and aminoxyacetic acid [90]. Of these, propargylglycine is the most common, as well as irreversible. Propargylglycine inhibition of CSE is achieved through the C γ of PAG covalently binding to Tyr114, forming a vinyl-ether. Several hydrogen bonds between adjacent subunits help to stabilize the ether. Interestingly, inhibition of CSE by PAG is only effective when the enzyme is breaking a C- γ -S sulfur bond, which requires a two-step mechanism. Both Tyr114 and Lys212 serve this purpose. When CSE is catalyzing the production of H₂S from cysteine, a one step-mechanism is required, and thus Lys212 is sufficient, ignoring Tyr114 [89].

Regulation of CSE is currently understudied. Phosphorylation of Ser377 has been linked to carbon monoxide dependent stimulation of protein kinase G (PKG). While this residue is buried, and the exact mechanism of phosphorylation is unknown, phosphorylation of Ser377 results in decreased H₂S production [91]. The presence of two CxxC motifs in CSE mark possible sites for regulation. One of which, Cys307-X-X-Cys310 is surface exposed, near the periphery of the enzyme, and at the end of an alpha-helix. The second motif, C252-X-X-Cys255 is more buried and located near the dimer-dimer interface and is present within an alpha-helix secondary structure.

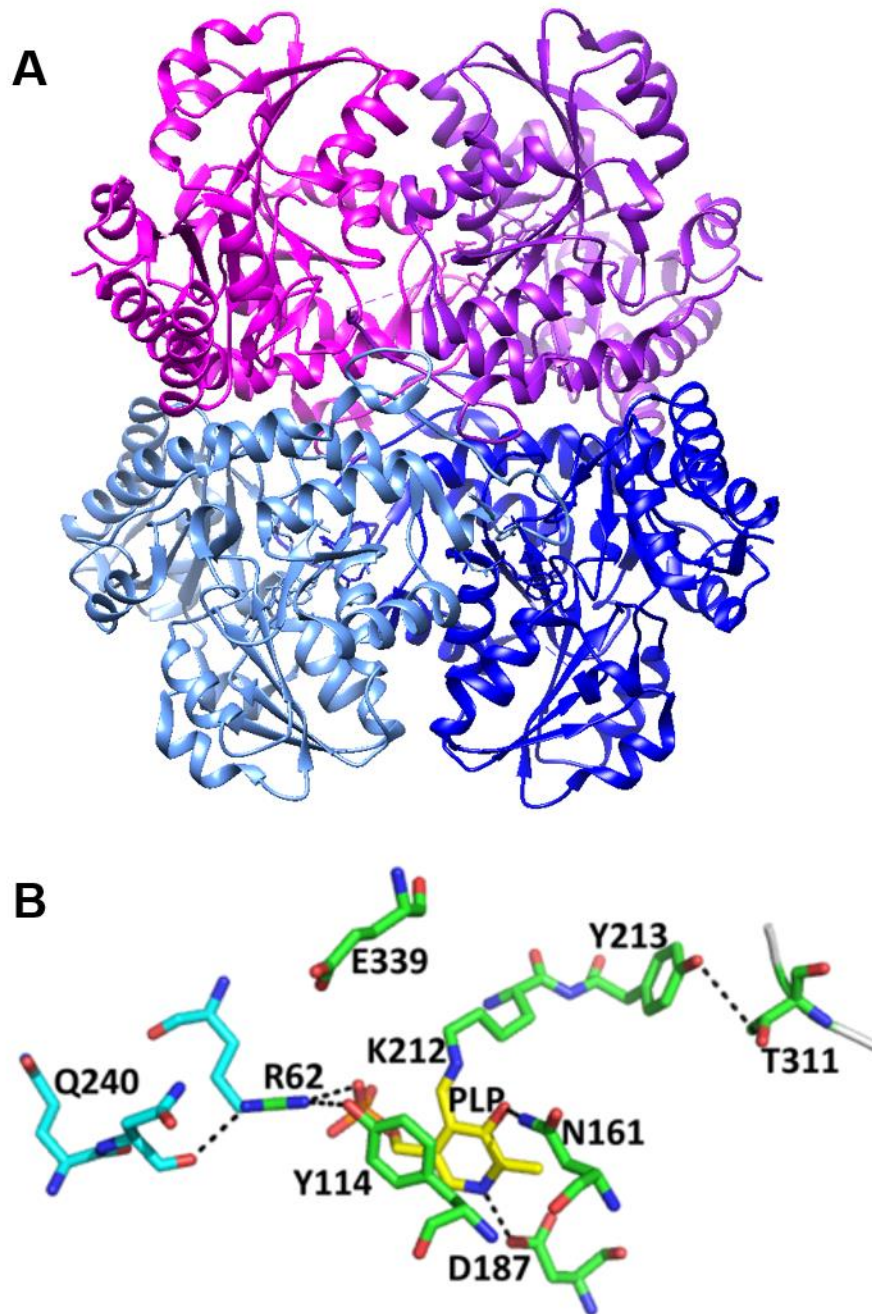


Figure 1.6 (A) Crystal structure of CSE. The four separate chains are highlighted in unique colours (PDB Code: 2NMP). (B) Active site of CSE showing key residues, including PLP (PDB Code: 2NMP).

1.3 CxxC Motif

A CxxC motif is characterized by two cysteine residues, intervened by two other, random residues that together form an active site. CxxC motifs are commonly associated with zinc binding in zinc finger binding domains [92]. In the thioredoxin superfamily of enzymes, of which protein disulfide isomerase and thioredoxin are members, the CxxC motif is the active site [93, 94]. These enzymes are involved in disulfide bond redox, shown in **Figure 1.7**. The proximity of the two cysteine residues allow for the reduction or oxidation of disulfide bonds. When the N-terminus of an alpha-helix points towards a cysteine residue, the electrostatics of that helix have been shown to lower the pK_a of said cysteine by up to 5 pH units [95]. This can be observed in the solvent exposed C307-X-X-C310 residue of CSE. This creates a nucleophile which is able to reduce an oxidized cysteine substrate, creating a disulfide intermediate. The C-terminal is then able to attack this newly formed intermolecular disulfide, reducing the product and forming an oxidized CxxC motif [95].

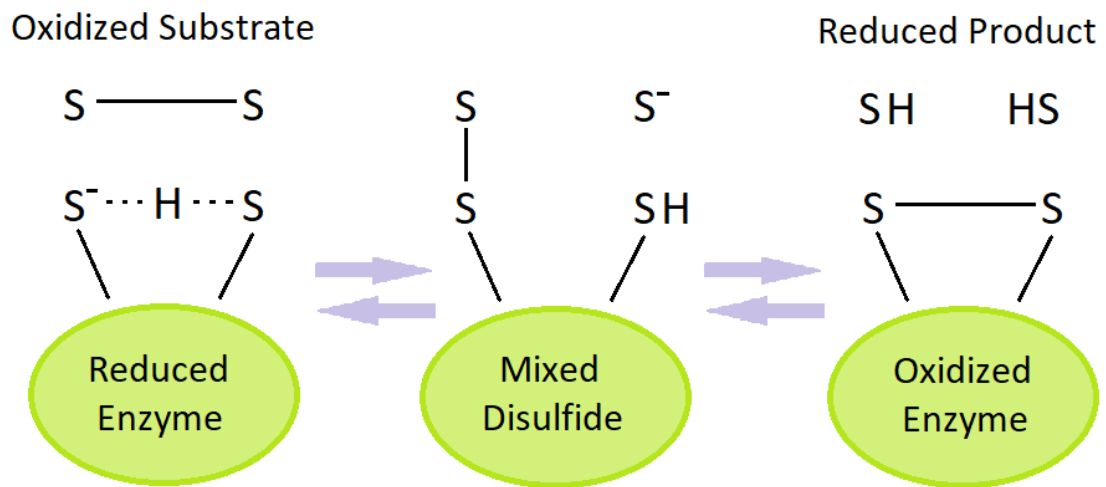


Figure 1.7 CxxC disulfide redox mechanism. The reduced enzyme is able to reduce the disulfide bond of the substrate forming a mixed disulfide intermediate. The N-terminal cysteine initiates a nucleophilic attack on the oxidized substrate, generating a reduced product and an oxidized enzyme.

1.4 Fluorogenic Free Thiol Probes

The phenomenon of fluorescence self-quenching (FSQ) occurs when two identical fluorophores are in close proximity to one another. Under this scenario, the intermolecular interactions between the two fluorophores quench the native fluorescence, which allows for the exploitation of this phenomenon for use in measuring enzymatic activity [96, 97]. The fluorescent pseudo-substrates developed for CSE are based off of the Di-E-GSSG fluorescent probe previously designed in the Mutus lab [96]. The developed probes utilize the fluorescent molecule fluorescein isothiocyanate (FITC) as the fluorophore, and the disulfide containing molecules cystine, homocystine and glutathione disulfide as the backbone. Nucleophilic attack from the amine of a backbone molecule on the S-C double bond of FITC results in the formation of a thiourea product, as shown in **Figure 1.8**. Each cystine amine is capable of nucleophilic attack, resulting in a product with two FITC moieties per cystine/homocystine/GSSG.

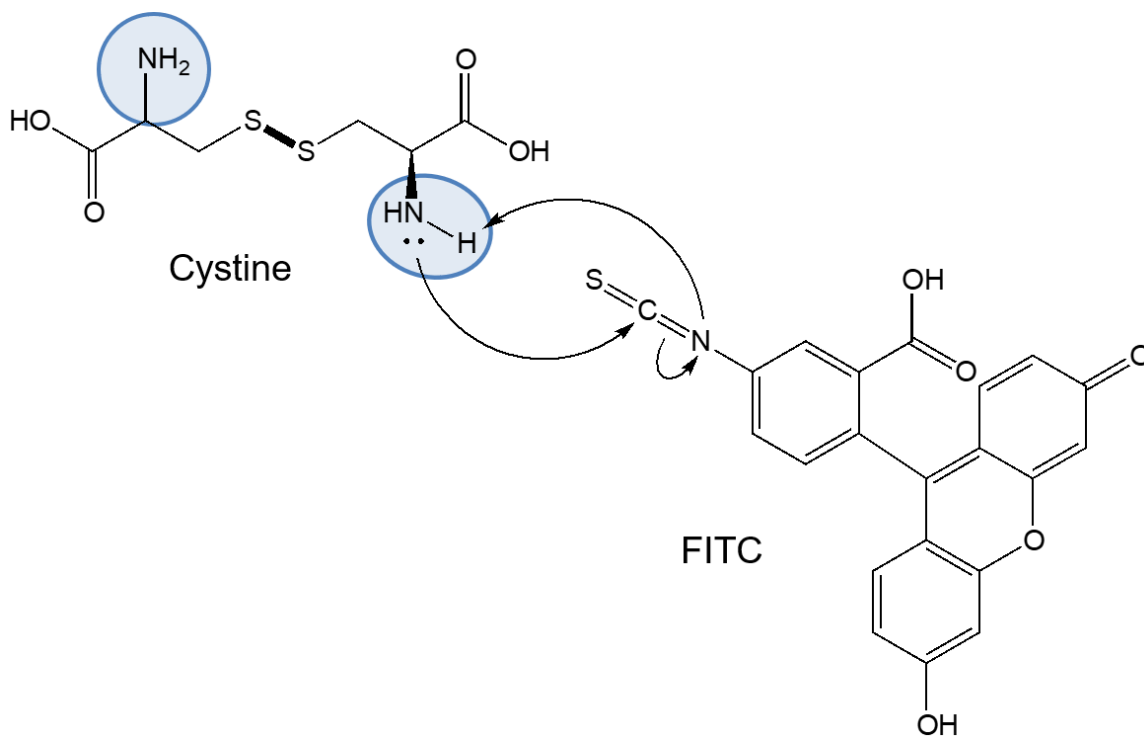


Figure 1.8 Synthesis of FITC₂-Cystine probe. Nucleophilic attack results in the formation of a thiourea.

1.5 Research Objective and Rationale

Hydrogen sulfide and reactive persulfides, both produced by the enzyme cystathionine γ -lyase, have been implicated in various signaling events throughout the body. While CSE and CBS are responsible for production of these two signaling molecules, regulation of CSE is not well understood, with only two post-translational modifications observed. The presence of two CxxC motifs of unknown function within each monomer of CSE, one of which meets criteria for a catalytic site is of interest. The CxxC motif is commonly associated with the thioredoxin superfamily of enzymes [93, 94].

The goal of this research project is to investigate and characterize the roles of the C₂₅₂-X-X-C₂₅₅ and C₃₀₇-X-X-C₃₁₀ motifs in CSE. Site directed mutagenesis was performed to investigate the individual effects of changing each or all cysteines to serines. The use of steady state kinetic assays discerned any loss or enhancement of enzymatic activity. Additionally, the use of fluorescent probes which are capable of reduction by CxxC motifs were synthesized to test the potential of these CxxC sites. Lastly, mass spectrometry was performed to detect any modification of CSE by the synthesized probe in an attempt to elucidate the residues responsible for this activity.

CHAPTER 2:
MATERIALS AND METHODS

2.1 Materials and Chemicals

Product	Distributor
Rosetta™ (DE3) pLysS <i>E. coli</i>	EMD Millipore
BL21 (DE3) <i>E. coli</i>	
BL21 (DE3) pLysS <i>E. coli</i>	
NEB® 5-alpha Competent <i>E. coli</i>	New England BioLabs
Q5® Site Directed Mutagenesis Kit	
BAMHI Restriction Endonuclease	
Formic Acid	
Imperial Stain	ThermoFisher
PageRuler Plus Prestained Protein Ladder	
Trifluoroacetic Acid	
Zeba™ Spin Desalting Columns	
Acetonitrile	
Ampicillin (Amp)	
Bacteriological Agar	
Bicinchoninic acid (BCA)	
Bovine Serum Albumin	
Chloramphenicol	
Copper (II) Sulfate	
Dialysis Tubing, 8k MWCO	
Dithiothreitol	Sigma Aldrich
DNase	
DTNB	
Ethidium Bromide	
Fluorescein-5-isothiocyanate	
Glutathione, oxidized	
Glutathione, reduced	
HIS-Select® Ni-Affinity Resin	

Iodoacetamide	
Isopropyl β -D-1-thiogalactopyranoside	
Kanamycin sulfate	
L-cystathionine	
L-cystine	
L-homocystine	
Lysozyme	
N-ethylmaleimide	
Phenol:Chloroform:Isoamyl Alcohol, 25:24:1	
Phenylmethane Sulfonyl Fluoride (PMSF)	
Propargylglycine	Sigma Aldrich
Pyridoxal-5`-phosphate	
Sephadex G-25	
Sodium Dodecyl Sulfate	
Tryptone	
Tween-20	
Yeast Extract	

Oasis HLB 1 cc Vac Cartridge	Waters
QIAprep Spin Miniprep Kit	Qiagen

2.2 Methods

2.2.1 Site Directed Mutagenesis

Mutagenesis of vicinal thiol residues Cys²⁵², Cys²⁵⁵, Cys³⁰⁷, and Cys³¹⁰ was performed using the Q5® site-directed mutagenesis kit (NEB). The primers used were designed in an end-to-end, or budding fashion, such that the mutagenic sequence that contained the amino acid substitution(s) was found in the forward sequence, resulting in an amino acid substitution of Cys to Ser. Polymerase Chain Reaction (PCR) conditions were separately optimized for each primer set (Appendix A). A Biorad ®T-100 Thermal Cycler was used to carry out 25 cycles of denaturation at 98 °C for 10 seconds, followed by primer annealing at varying temperatures (Appendix A), for 30 seconds, and plasmid elongation and extension at 72 °C for 4 and a half minutes. The PCR products were treated with a kinase-ligase-DpnI (KLD, NEB®) as per the provided instructions. KLD treated product was screened on a 1% agarose gel to ensure the presence of banding. Successful PCR reactions resulted in the transformation of the respective plasmid into NEB ® 5-alpha competent *E.Coli* (High efficiency) using the heat-shock method as per manufacturer instructions. Transformed cells were plated on 2 x YT LB agar plates containing 50 µg/mL of the antibiotic kanamycin and grown overnight at 37 °C. Individual colonies were selected and grown overnight in liquid LB-Kan. The resultant bacterial growth was then used for plasmid isolation *via* a standard phenol-chloroform extraction (Qiagen, see 2.2.2). Extracted plasmids were sequenced by Robarts's Research Institute (London Regional Genomics Center, London, Ontario, Canada) to ensure the successful mutations as well as the presence of the hCSE gene in the pET-28b(+) vector. The mutations resulted in the following mutants; C252S, C255S, C307S, C310S, double mutants C252S_C255S, C307S_C310S, and quadruple mutant C252S_C255S/C307S_C310S.

2.2.2 *Plasmid Miniprep*

Plasmid DNA isolation from *E. Coli* was adapted from a standard protocol (Qiagen). Briefly, 1.5 mL of previous *E. Coli* culture was centrifuged at 12,000 x g for 1 minute. The resultant pellet was resuspended in 100 µL of buffer P1 (50mM glucose, 25mM TRIS-HCL pH 8.0, 10mM EDTA). 200 µL of Buffer P2 (0.2M NaOH, 1% SDS) was added to the resuspended pellet and inverted to mix. To this, 150 µL of Buffer P3 (3M NaOAC, pH 5.2) was added and incubated on ice for 30 min, before centrifugation at 12,000 x g for 10 min. 500 µL of phenol:chloroform:isoamylalcohol was added to the collected supernatant, vigorously shaken and centrifuged at 12,000 x g for 30 seconds. The top aqueous layer was removed and 500 µL of chloroform was added, shaken vigorously and centrifuged again at 12,000 x g for 30 seconds. The aqueous phase layer was then collected and 900 µL of anhydrous EtOH was added. Sample was inverted to mix and immediately centrifuged at 12,000 x g for 2 minutes. The EtOH was aspirated, and the resultant pellet was washed with 70% EtOH, dried, and reconstituted in 30 µL of TE buffer.

2.2.3 *Bacterial Plasmid Transformation*

WT and mutated hCSE plasmid products were transformed *via* the heat-shock method. Briefly, *WT* and mutated hCSE plasmid products (5 µL) were added to 25 µL of competent *E. Coli* BL21 (DE3) (New England Biolabs) and incubated on ice for 30 minutes, followed by a 45 second heat shock at 42 °C, then returned to ice for 5 minutes. 950 µL of RT SOC media was added to the transformed cells and incubated with shaking at 37 °C for one hour. The incubated culture was then plated onto LB-agar (50 µg/mL kanamycin A, 25 µg/mL chloramphenicol) and grown for 16 hours at 37 °C while shaking.

2.2.4 Purification of CSE

The protocol described below was followed for *WT* as well as all previously mentioned mutant constructs of hCSE. Successfully transformed cells were grown at 37 °C, shaking, overnight in 100 mL 2xYT media containing kanamycin A (50 µg/mL). This overnight culture was used to inoculate 1L of fresh 2xYT (kanamycin A) and grown at 37 °C, shaking, until a cell density (OD₆₀₀) of 0.7-0.8 was achieved. To induce protein expression, 1mM IPTG was added and incubated at RT for 20 hours. Cells were collected *via* centrifugation at 6, 000 rpm for 30 min at 4°C. Resultant pellets were resuspended in 10 mL, pH 8.0 Lysis Buffer (100 mM NaCl, 50mM Tris-HCl, 2mM EDTA, 2mM PMSF, 1% Triton X-100, 100 µg/mL lysozyme, 50 µg/mL DNase 1) and incubated on ice for 30 minutes. Following incubation on ice, the cell debris underwent sonication on level 5 for 8 cycles of 30 seconds (Sonic Dismemberator, Fisher Scientific) on ice. Cellular debris was further separated *via* centrifugation at 12, 000 rpm for 30 minutes at 4°C. The supernatant was applied to a previously equilibrated (40 mM Tris-HCl, pH 8.0) HIS-Select™ Nickel Affinity resin with a column volume of 5 mL. The resin was subsequently washed with 10 column volumes of wash buffer (50mM Tris-HCl, 40 mM Imidazole, pH 8.0). His-tagged hCSE was eluted with 2 column volumes of an elution buffer containing 50 mM Tris-HCl, 250 mM Imidazole, pH 8.0. Eluted protein was buffer exchanged over a period of 20 hours at 4°C *via* dialysis and previously prepared dialysis tubing (Sigma). Dialysis buffer contained 100mM potassium phosphate, 2mM EDTA, and 50 µM PLP, pH 8.0. Buffer was changed twice, at the 2- and 14-hour marks. Protein purity was assessed *via* SDS-PAGE (See **Appendix , Figure A1**) and concentration *via* BCA assay [98].

2.2.5 *In Vitro Kinetic Assays*

All kinetic assays were performed at room temperature ($\sim 22 \pm 2$ °C) using fresh enzyme. Any assays utilizing mutant enzyme were performed in triplicate and in parallel with *WT* enzyme or an untreated control to ensure both consistency and validity in the results. All UV-VIS experiments were performed on an 8453 UV-VIS Spectrophotometer (Agilent Technologies, Mississauga, ON). All fluorescent experimental data was collected by a Cary Eclipse fluorescence spectrophotometer using a 5nm slit width and medium gain settings.

2.2.5.1 *Cystathionine Catabolism Assay*

L-cystathionine was the chosen substrate to elicit the steady-state catalytic parameters of CSE. Ellman's Reagent (DTNB) was the chosen probe to track the formation of the L-cysteine product through the formation of 2-nitro-5-thiobenzoate (TNB²⁻), a product with a characteristic absorbance at 412nm. Excess DTNB (100 μ M) was added to a 500 μ L cuvette containing varying concentrations of 0.1-5.0 mM L-cystathionine in the standard CSE reaction buffer (100 mM phosphate, 2mM EDTA, pH 8.0). Reaction components were allowed a 30 second period for equilibration before CSE was added and mixed to a final concentration of 300 nM. The initial rate of reaction was determined from the linear slope of the first 60 seconds. The molar extinction coefficient of DTNB, in conjunction with the Beer-Lambert Law, allowed for the determination of Michaelis-Menten kinetic parameters [99]. Kinetic data was fitted to a Michaelis-Menten like hyperbolic curve (*Equation 2.1*) using the *Solver* function in *Excel*.

$$V_o = \frac{V_{max}[S]}{K_M + [S]}$$

Equation 2.1

2.2.5.2 pH Gradient

To determine the optimum pH for the activity of CSE, a single concentration of L-cystathionine (1.5 mM), was made in CSE assay buffer at a range of pH (6.0-9.0). As per the catabolism assay, the linear slope of the initial 60 seconds was used to determine Michaelis-Menten parameters. The resultant data was plotted in *Excel* where the optimum operating pH was visualized. This was repeated with all mutant enzymes, to determine any effect on optimum pH.

2.2.5.3 Free-thiol Determination Assay

CSE free thiol determination involved the usage of Ellman's Reagent and CSE assay buffer without a substrate present. Four different concentrations (0.25, 0.5, 0.75, 1.0 $\mu\text{g}/\mu\text{L}$) in triplicate were incubated in an excess amount of 10 mM DTNB (10 μL) and varying amounts of buffer to make the reaction volume. The reactions were incubated at 4 $^{\circ}\text{C}$ and placed on a shaker for 30 min, and their absorbance at 412nm recorded. Using the provided extinction coefficient of $14140^{-1} \text{ cm}^{-1}$, the number of solvent accessible free thiols per μL could be obtained[100].

Denaturation of the CSE to determine total free thiol content was performed *via* incubation of CSE in 6M Guanidine Hydrochloride (GHC1) for 1 hour at 4 $^{\circ}\text{C}$, with shaking. Samples were desalted, and buffer exchanged to CSE assay buffer using Zeba™ Spin Desalting columns (ThermoFisher Scientific, Waltham, MA, USA) as per the manufacturer's instructions. The above protocol was followed to determine total free

sulfide content.

2.2.5.4 *Oxidation of CSE*

Oxidation of CSE was performed using Glutathione disulfide (GSSG). GSSG was added in excess of 20-100-fold over the free thiol content in *WT* CSE. Samples were incubated for 1 hour at 4 °C, shaking. Excess GSSG was removed using Zeba™ spin columns, as described above. Oxidized CSE was used in an L-cystathionine catabolism assay as earlier stated.

2.2.5.5 *S-Nitrosylation of CSE*

Tenfold molar excess of prepared S-Nitrosoglutathione (GSNO) was added to CSE. GSNO was prepared by Dr. Bulent Mutus, University of Windsor, Windsor, Ontario, Canada. Briefly, 1.5g of glutathione (GSH) was dissolved in 15 mL ice cold water. To that, 25 mL 2M HCl was added, followed by 0.345g of NaNO₂. Mixture reacted at 4 °C for 40 minutes, 10 mL acetone added, followed by 10 minutes more reaction time. Resultant paste was vacuum filtered, washed 3 times with 10 mL acetone, and 3 times with 10 mL water. Product was lyophilized until powder form. CSE/GSNO reacted for one hour at 4 °C, shaking. Excess GSNO was removed using Zeba™ spin columns, as described above. S-nitrosylation effects on CSE were observed *via* a cystathionine catabolism assay, as described previously.

2.2.5.6 *Fluorescent Probe Kinetics*

Di-Eosin glutathione disulfide (Di-E-GSSG) was synthesized by Cody Caba of the Mutus group (University of Windsor, Windsor, Ontario, Canada). Mitchell DiPasquale of the Mutus group (University of Windsor, Windsor, Ontario, Canada), performed the Di-E-GSSG kinetics utilizing *WT* enzyme, as well as the quadruple, 300 double, and 200 double

mutants. Leslie Ventimiglia of the Mutus group (University of Windsor, Windsor, Ontario, Canada), performed preliminary fluorescent probe kinetic analysis on the FITC₂-Cystine, FITC₂-Homocystine, and FITC₂-GSSG using the WT, 200, 300, and quadruple mutants.

2.2.5.6.1 *Di-Eosin Glutathione Disulfide*

Di-E-GSSG was used as a possible fluorescent disulfide pseudo substrate for CSE. Varying concentrations of Di-E-GSSG (0.1-4.0 μM) was added to CSE assay buffer in a 500 μL skirted cuvette. A 60 second initial reaction time with excitation and emissions of 525 and 545 nm respectively was used to determine a baseline. Both CSE (including above stated mutants) and inhibited CSE was added to a final concentration of 500 nM, where EGSH formation was measured as an increase in fluorescence at 545 nm. A Di-E-GSSG standard curve permitted the quantification of relative fluorescence to that of product concentration. This allows for the expression of the rate of EGSH production to be characterized by Michaelis-Menten kinetics.

CSE was inhibited by the addition of 1mM propargylglycine (PAG) to CSE stocks. The mixture was carried out under shaking at 4 °C, for 1 hour. PAG is a known, and common inhibitor of CSE [101].

2.2.5.6.2 *Synthesized FITC Probes*

Initial CSE fluorescent assays were performed with 5 concentrations (0.25-5.0 μM) of the 3 synthesized probes added to a 500 μL skirted cuvette containing CSE assay buffer. Excitation and emission of 494 and 521nm were used to obtain a baseline after 30 seconds. CSE was added to a final concentration of 10 μM and allowed to react in the cuvette for 90 seconds. Subsequent CSE fluorescent assays were performed with 7 concentrations (0.1-5.0μM) of only FITC₂-Homocystine. FITC₂-homocystine was also tested with all

available mutants.

2.2.6 *Probe Synthesis and Purification*

2.2.6.1 *Probe Synthesis*

The following synthesis was prepared with the help of Leslie Ventimiglia of the Mutus group (University of Windsor, Windsor, Ontario, Canada). The below protocol was followed for synthesis of FITC₂-Cystine (FITC-Cys), FITC₂-Homocystine (FITC-Homo), and FITC₂-Glutathione disulfide (FITC-GSSG). The protocol describes the FITC-Cys synthesis. For synthesis of FITC-Homo or FITC-GSSG, L-cystine was replaced with homocystine or glutathione disulfide respectively. Reaction of L-cystine and fluorescein isothiocyanate (FITC) occurred on a small scale, 6 mL. Sodium carbonate (Na₂CO₃, 0.3M) was dissolved in 3 mL Mili-Q H₂O, followed by 3 mL 99.5% acetone; solution was left to react until homogenous. 0.2 M L-cystine was added and left to dissolve at 50 °C. To the dissolved cystine, FITC was added in a 2.5:1 molar ratio with L-cystine and left to react at 50 °C, stirring, and wrapped in parafilm and foil to protect from light exposure. Fluorescent activity of the crude product was confirmed using a fluorometer set to an Excitation and Emission of 494 and 521 nm respectively. Briefly, 1 µL crude product was added to a skirted 500 µL containing 5 µL 1M DTT and 494 µL CSE assay buffer, pH 8.0. Product was snap frozen at -80 °C and lyophilized until a dry powder, where it was stored at -20 °C until size-exclusion chromatography could be performed.

2.2.6.2 *Probe Purification*

Lyophilized probe was purified *via* Sephadex® G-25 gel chromatography. G-25 resin was swelled in excess ddH₂O overnight, and subsequently packed into a 3cm by 30 cm column with a constant flow of ddH₂O supplied by an Econo Pump (Bio-Rad Labs).

Dry, crude, probe was reconstituted in as little 0.5 M phosphate buffer (pH 8.5) as possible, generally 3-4 mL, and added to the dry G-25 column bed. Probe was allowed to diffuse into the column where a constant flow of ddH₂O was provided to elute the probe over time. The elution was monitored for absorbance changes overtime using the BioLogic LP UV-VIS and subsequent software. Fractions were collected when a change in absorbance was detected, and collection ceased once the absorbance returned to a baseline. Fractions were frozen at -80 °C and lyophilized until a dry powder was reached. The purified probe was resuspended in as little 0.1M phosphate buffer as possible. Concentration was determined using UV-VIS at a wavelength of 494nm, and Beer Lambert Law with the ϵ 88,000 M⁻¹cm⁻¹ of FITC. Reported concentrations were halved in accordance with the two FITC present per molecule of cystine.

Fold-increase of the purified probe was determined using methods stated above.

2.2.7 Fluorescent Labelling of CSE

CSE was fluorescently labelled and visualized using an SDS-PAGE system. The samples to be labelled and visualized were modelled off the fluorescent kinetic experiments. The final amounts of both probe and enzyme were held constant from the reactions in the cuvettes. Two main gel sample combinations were used during these experiments.

2.2.7.1 Fluorescent Probe and All CSE variants

The below protocol was repeated for each of the 4 available fluorescent probes: FITC₂-Cystine, FITC₂-Homocystine, FITC₂-GSSG, Di-E-GSSG, and the overall experiments were repeated in triplicate.

CSE and CSE mutants (255, 252_255, 307, 310, 307_310, Quad) were added to a microcentrifuge tube containing CSE assay buffer, plus 1mM PMSF, to a final concentration of 1.8 μ M, or 30 μ g of protein. To this, FITC₂-Cystine was added to a final concentration of 5 μ M and total reaction volume of 300 μ L. The prepared samples reacted at RT for 2 hours with gentle shaking, protected from the light. 5x, non-reducing SDS sample buffer was added to 25 μ L of reacted samples and boiled. Samples were run on a 12% SDS gel until the sample buffer dye front ran off, about 2 hours. Gels were rinsed with Mili-Q before imaging using a FluoroChem® Q quantitative imaging system (Alpha Innotech) using the CY2 function. Gels were then stained and visualized using Coomassie, to ensure an equal amount of protein was loaded.

2.2.7.2 All CSE Variants with DTNB Thiol Blocking

The below protocol was repeated for 7 of the 8 available CSE constructs (production and purification issues of the single 252 CSE mutant), and the overall experiments were repeated in triplicate.

WT CSE was added to a final concentration of 1.8 μ M or 30 μ g to 8 microcentrifuge tube containing CSE assay buffer, as stated above. DTNB was selectively added to every other tube as a thiol blocker to a final concentration of 0.33 mM. The CSE/DTNB mixture reacted for 2 hours with gentle shaking at RT. To two of these tubes, 5 μ M FITC₂-Cystine was added. Likewise, the remaining probes (FITC₂-Homocystine, FITC₂-GSSG, Di-E-GSSG) were added to the remaining tubes resulting in each probes exposure to WT CSE and a thiol-blocked WT CSE. These mixtures then reacted at RT with gentle shaking for 2 hours. As stated above, samples were run on 12% SDS gels and fluorescently imaged, then stained by Coomassie to visualize equal loading of protein.

2.2.8 *Mass Spectrometry*

2.2.8.1 *High Performance Liquid Chromatography Electrospray Ionization Mass Spectrometry (HPLC-ESI MS)*

A random gel piece was digested following the same protocols as outlined below to act as a control. Fluorescently labelled hCSE (FITC₂-homocystine treated) were ran in tandem with a duplicate Coomassie stained gel to ensure presence of fluorescence on CSE prior to digestion. *WT* CSE as well as the 307 and 310 cysteine to serine mutants were digested.

2.2.8.1.1 *Proteolysis and Sample Preparation*

Digestion of both CSE and modified CSE was performed using a modified version of an established in-gel trypsin digestion protocol [102]. For CSE and CSE mutants, 5 µg was run on a 12%, non-reducing SDS gel until the dye front ran off. Protein was visualized with Imperial™ Protein Stain (ThermoFisher Scientific), and destained with Mili-q H₂O until clear. Bands of interest were excised with a clean scalpel and placed in a siliconized microcentrifuge tube. Excise bands were cut into 1 x 1 mm squares in the tube. Excised bands were destained using fresh 100 µL 50 mM ammonium bicarbonate (ABC) made in Mili-q and 100% acetonitrile (ACN) in a 1:1 (vol/vol) solution. Gel pieces were incubated with shaking at 37 °C for 15 minutes, destain was decanted and fresh destain was added and the process was repeated. 400 µL of neat ACN was added to the decanted gel piece and left for 5-10 minutes with occasional vortexing. Samples were dried using a Digital Series SpeedVac™ Systems in combination with a Savant RVT5105 Ultra-Low Temperature Refrigerated Vapor Trap (ThermoFisher Scientific) until the gel pieces shrunk and turned white. Lyophilized Trypsin G old, Mass Spectrometry Grade (Promega)

was resuspended in provided resuspension buffer and brought to a working concentration of 13 ng/ μ L through the addition of 100 μ L 50 mM ABC. 30 μ L trypsin was added to the dry gel pieces and allowed to sit on ice for 30 min. Additional trypsin was added if required to saturate the gel pieces, generally an additional 30 μ L of trypsin, and left to sit for 90 minutes. ABC was added (20-30 μ L) to cover gel pieces and keep wet during digestion. Samples were shaken overnight (16 hours) at 37 °C to allow for complete digestion. Samples were decanted, and pre-extract saved. Tryptic peptides were extracted using 200 μ L extraction buffer (1:2 (vol/vol) 5% formic acid (FA)/100% ACN) with shaking at 37 °C for 15 minutes; repeated twice while collecting the extract after each incubation. Extracted peptides were dried once again. Dried peptides were reconstituted in 100 μ L 0.1% trifluoroacetic acid (TFA) for sample cleanup and desalting using Oasis HLB 1 cc Vac Cartridges according to manufacturer's instructions. Desalted peptides were dried and resuspended in 25 μ L 0.1% FA for ESI-MS analysis.

Modified CSE involved the incubation of CSE with either FITC₂-Homocystine or homocystine prior to SDS-PAGE. Fluorescent sample preparation was similar to the described method in *section 2.2.7.1* with 10 μ M FITC₂-Homocystine or 100 μ M homocystine addition. Modified samples were quenched prior to separation *via* SDS page using a cold acetone precipitation procedure. Four times sample volume of ice-cold acetone was added, vortexed and incubated at -20 °C for 1 hour. Samples were spun down at 12,000 x g for 10 minutes. Acetone was aspirated, and pellets were allowed to air dry for 20 minutes before resuspension in buffer. Modified CSE samples were then digested as per the protocol described above.

2.2.8.1.2 *Data Acquisition*

Mass Spectrometry was performed by Dr. Janeen Auld (University of Windsor, Windsor, Ontario, Canada).

Prepared samples were analyzed using a Waters SYNAPT G2-Si time-of-flight mass spectrometer configured for nano-ESI operated in positive-ion mode coupled to a Waters nanoACQUITY UPLC system. The UPLC was configured for 1D single pump trapping. Mobile phase buffer A was 0.1% formic acid. Mobile phase buffer B was acetonitrile with 0.1% FA. Samples were loaded onto the column in 97% buffer a and 3% buffer B over 3 minutes and flow rate of 5 μL per minute. A 7-step, 60 min gradient run at 0.3 μL per minute. Buffer A concentration at 5 minutes was 90%, 75% at 15 minutes, 50% at 22 minutes, 25% at 41 minutes, 15% at 42 minutes, 15% at 44 minutes and finally 97% at 45 minutes. Samples were analyzed in MS^{e} mode followed by data processing with Progenesis QI.

2.2.8.2 *Holo-enzyme Mass Spectrometry*

2.2.8.2.1 *Sample Preparation*

Prepared CSE (80 μg) was added to a microcentrifuge tube containing 150 μM homocystine as well as CSE assay buffer. The mixture reacted for 15 minutes with gentle shaking at RT. Resultant mixture was snap-frozen in liquid nitrogen before freeze drying could occur *via* a lyophilizer. The dried protein was reconstituted in 80 μL H_2O ; 5 μL of resuspended solution was mixed with 295 μL 0.1% formic acid.

2.2.8.2.2 *Data Acquisition*

Mass Spectrometry was performed by Dr. Yufeng Tong ((University of Windsor, Windsor, Ontario, Canada). Prepared samples were analyzed using an Agilent Q-ToF 6545

LC/MS.

2.2.9 Molecular Modelling

Molecular modelling was performed by Dr. Bulent Mutus (University of Windsor, Windsor, Ontario, Canada). Predicted molecular structures for each of the fluorescent free thiol probes, as well as respective MM2 energy minimizations were created using ChemDraw 3D.

2.2.10 Statistical Analysis

One-way ANOVA followed by Dunn's multiple comparison test, as well as Two-way ANOVA were performed using GraphPad Prism version 7 (GraphPad Software, La Jolla California, USA).

CHAPTER 3:
RESULTS

3.1 Site Directed Mutagenesis

A total of seven hCSE mutants were designed and purified. Successful mutagenesis was confirmed *via* cDNA sequencing. These cysteine residues were targeted due to their lack of overall study. Specifically, each cysteine was mutated to a serine using primers defined in **Appendix A, Table A.1**. A cysteine to serine mutation was chosen due to the overall minor impact the change would induce, as both amino acids are polar and uncharged. Overall, mutant hCSE variants produced included single mutants C252S, C255S, C307S, and C310S, double mutants C252S_C255S and C307S_C310S, and lastly a quadruple mutant C252S_C255S_C307S_C310S. The purity of the isolated enzymes was assessed using SDS-PAGE (**Appendix A Figure A.3**). Hereinafter, the C252S_C255S and C307S_C310S will be referred to as the 200 double and 300 double mutants respectively, while the single mutants will be named as they are, ex, C252S. Likewise, the C252S_C255S_C307S_C310S mutant will be referred to as the quad.

3.2 *In-vitro* Kinetic Assays

In order to assess the potential effects that the mutation of each cysteine involved in the CxxC motif to serine have upon the enzymatic activity, a cystathionine catabolism assay was performed. The Michaelis-Menten profile of the mutants were determined using a constant concentration of DTNB, while varying the concentration of cystathionine. Prior to the cystathionine catabolism assay, the stability of DTNB was tested at various pH values (not shown). DTNB begins to breakdown at pH values greater than 7, however stability is increased in phosphate buffer until pH values greater than 8 [76]. DTNB was shown to be stable in CSE activity buffer, but, nevertheless a blank rate which included DTNB, CSE assay buffer and L-cystathionine was subtracted from any enzymatic rate to

ensure the faithfulness of the data.

The *WT* enzyme and the mutants displayed a great variance in the ability to catabolize L-cystathionine, as seen in **Figure 3.1**. Specifically, the *WT* as well as the C307S and C310S exhibited remarkably similar Michaelis-Menten profiles. This is further shown in the extracted kinetic parameters, displayed in **Table 3.1**. All three constructs share the same K_M of 1.35 mM, and the indicators of enzymatic efficiency k_{cat} and k_{cat}/K_M are similar as well, indicating that the mutation of each individual cysteine in the 300 CxxC motif display little effect on the catalytic activity of the enzyme, with respect to cystathionine. The C252S mutation completely alters the activity of the enzyme, in essence it is catalytically and enzymatically deadinactive, with no detectable activity. The C255S mutation reports a similar K_M as the *WT*, but displays 62% of both the catalytic activity and catalytic efficiency of the *WT*. The 200-double mutant, like the C252S is devoid of all enzymatic activity with respect to cystathionine catabolism. The 300-double mutant, however, displays an identical K_M to that of the *WT*, but once again displays altered catalytic rate and efficiency values, possessing 21 and 22% of the *WT* values respectively. The quad mutant shows complete loss of catabolism of cystathionine activity as well.

The oxidation/reduction of CSE, as well as S-nitrosylation effects are shown in **Appendix B, Figure B.1**. The oxidation/reduction of *WT* CSE was performed by incubating *WT* with both GSH as well as GSSG. **Appendix B, Figure B.1 A** shows the lack of effect that both GSH and GSSG have on the CxxC motif, as well as any other free cysteines on the *WT*. Additionally, **B** shows the S-nitrosylation of CSE by GSNO. GSNO modifies thiols with a NO group. Both free thiols and the CxxC motifs should be targets of s-nitrosylation, but, as seen in **Appendix B, Figure B.1 B**, no effect on the rate of

cystathionine catabolism by both *WT* and C307S_C310S is observed.

Each CSE monomer contains a total of 10 cysteines, four involved in each CxxC and 6 additional residues. DTNB was used to determine the number of free thiols relative to the concentration of CSE in a solution. The number of free thiols in the native state, as well as the number of free thiols in the denatured enzyme were determined. In the native state, CSE has 44 μM of free thiol, with an enzyme concentration of 22 μM , indicating two free thiols. When denatured, CSE has 111 μM of free thiols, indicating that there are 5 free and accessible thiols present.

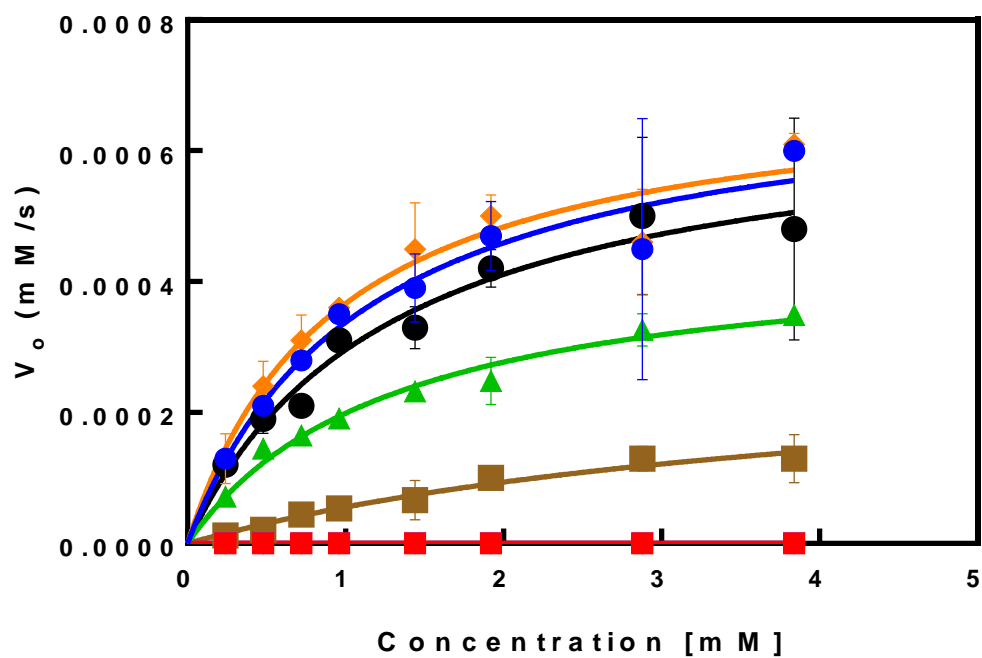


Figure 3.1 Catabolism of L-cystathionine of WT and mutants (WT, blue; C252S, red; C255S, green; C252S_C255S, purple; C307S, orange; C310S, black; C307S_C310S, brown; quad, purple). Varying concentrations of cystathionine (0.1-4 mM) were incubated with constant CSE and DTNB concentration; data reported as the mean \pm S.D. of $n = 3$ experiments.

Table 3.1. Extracted kinetic parameters of all CSE constructs seen in **Figure 3.1**.

CSE	WT	252	255	252_255	307	310	307_310
K_M (mM)	1.35	0	1.35	0	1.35	1.35	1.35
Vmax (mM/s)	0.00075	0	0.000465	0	0.00077	0.00069	0.000162
k_{cat} (s-1)	0.85	0	0.53	0	0.87	0.78	0.18
k_{cat}/K_M (mM-1s-1)	0.63	0	0.39	0	0.64	0.58	0.14

3.3 pH Dependent Activity of CSE Mutants

The pH-dependent activity profiles for each CSE construct that displayed enzymatic activity were tested at a single cystathionine substrate concentration (1.5 mM) over a varying pH range (6.0-9.0). The C252S, 200-double, and quad were not tested as the change in pH was not sufficient to recover enzymatic activity. In addition, accurate kinetic parameters could not be extracted from the data as multiple concentrations per pH value would be required.

The resultant pH curve for CSE constructs can be seen in **Figure 3.2**. All enzymes exhibited their lowest activity at pH 6, the lowest tested. The *WT* and C310S both exhibit a characteristic bell curve, with the maximal enzymatic activity reported at pH 7.8. The C307S and C255S mutants appear to exhibit a bell curve-like activity profile, but without additional data points it cannot be concluded. C307S exhibits maximal enzymatic activity at 8.6, while C255S shows maximum pH dependent activity at 8.3.

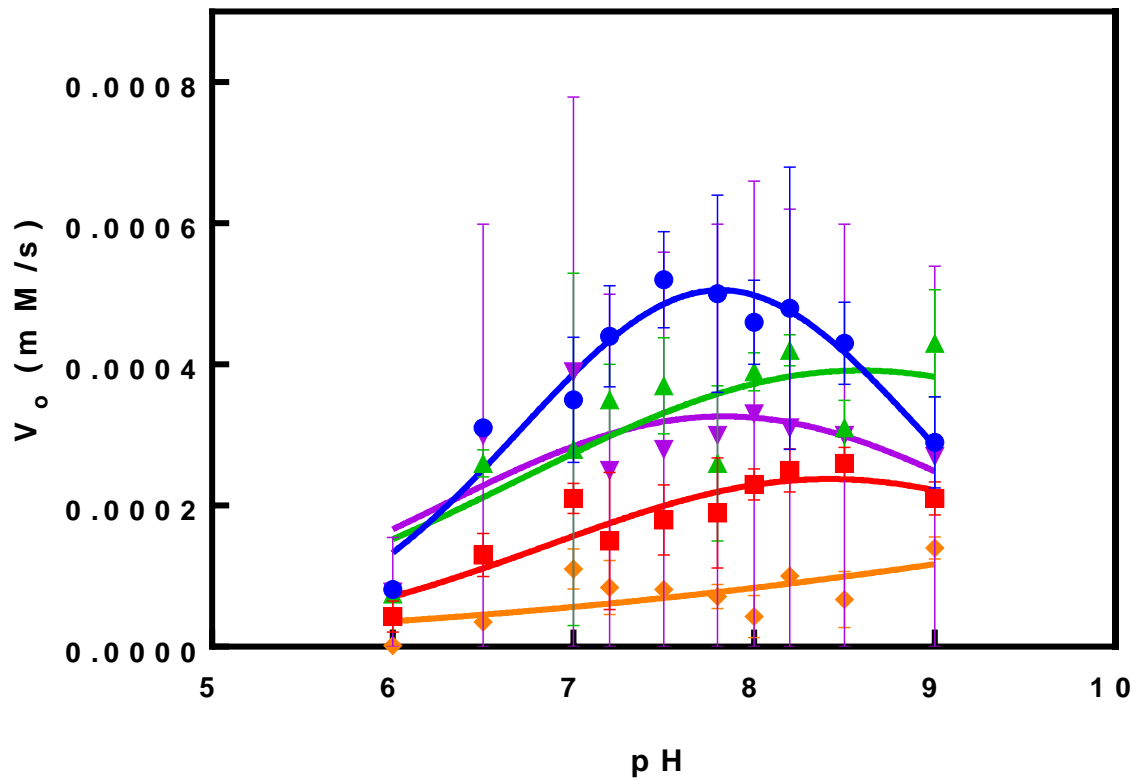


Figure 3.2 pH-dependent cystathionine catabolism activity profiles of CSE and CSE mutant constructs. (WT, blue; C255S, red; C307S, green; C310S, purple; C307S_C310S, orange). 1.5 mM cystathionine was incubated with constant enzyme and DTNB in CSE assay buffer of varying pH. pH profiles represent the mean \pm S.D of $n = 3$ experiments.

3.4 Di-E-GSSG as a CSE Pseudo Substrate

Prior work in the Mutus lab established Di-E-GSSG as a suitable substrate to monitor reaction kinetics as the PDI active site consists of two CXXC motifs [96]. The presence of the two CXXC motifs on CSE was the determining factor in the testing of Di-E-GSSG with CSE. The reaction of Di-E-GSSG with CSE led to a few interesting findings, which can be seen in **Appendix B, Figure B.2 A**. First, a kinetic rate was observed for the *WT*, 200-double, and 300-double, while no rate was observed for the quad mutant. The observation of a kinetic rate for the 200-double mutant is interesting as this is the first observation of some form of rate with this mutant thus far. A presence of a rate here indicates a possibility that this rate is independent of the active site of the enzyme. The **B** panel presents another noteworthy finding. The summation of the observed rates for the 200 and 300 double mutants are relatively equal to that of the *WT*, further supporting the notion that these rates are independent of the active site and are in fact the result of the CxxC motifs. Panels **C** and **D** further solidify the observed activity as independent of the active site. Panel **C** shows the successful inhibition of CSE by PAG. PAG is a useful inhibitor when the substrate requires a two-step mechanism, of which homocystine utilizes. Panel **D** shows both the same *WT* and PAG-inhibited CSE reacting with Di-E-GSSG, in which the observed inhibited rate matched identically to the *WT*. These results support an independent catalytic site outside of the traditional active site of CSE.

3.5 Novel Fluorescent Free Thiol Probes

The results shown above were the driving force for the design and synthesis of more suitable fluorescent free thiol probes to be used with CSE. Fluorescein was chosen as the fluorophore as it is a more economical alternative to eosin. The backbones of the free thiol

probes were chosen due to their role as disulfide containing alternative substrates for CSE, or as a key molecule in the transsulfuration pathway. While NMR provided inconclusive results due to both probe production, as well as concentration issues, the proposed structures shown in **Figure 3.3** are supported by FSQ. The fold increase displayed by each of the three synthesized probes indicates FSQ. **Figure 3.3 A** is FITC₂-cystine which, when incubated with 1M DTT showed a 10-fold increase in fluorescence. FITC₂-GSSG, shown in panel **B**, displayed a 12-fold increase after reduction by DTT. Lastly, FITC₂-homocystine exhibited a nearly 20-fold increase in fluorescence after reduction by DTT.

The suitability of each free thiol probe to monitor CSE CxxC activity was examined in a manner similar to that of the Di-E-GSSG probe, the results of which can be shown in **Figure 3.4**. Of the three synthesized probes, only FITC₂-homocystine showed some form of activity with CSE. Both FITC₂-cystine and FITC₂-GSSG show no activity with respect to the canonical active site of CSE or the CxxC motifs. FITC₂-homocystine activity was then examined with each of the available CSE mutants. It should be noted that production and purification issues of the C252S mutant did not allow for further testing of this construct. **Figure 3.4 B** shows FITC₂-homocystine activity with each of the mutants. The mutant kinetics provides some interesting results. Most noteworthy is the lack of activity of the quad mutant, solidifying the role of the CxxC in catalyzing disulfide bond cleavage. Of the singly mutated residues, the C310S displays the lowest rate. This is of interest as C310S is the most solvent exposed of all the cysteine's involved in a CSE CxxC motif. This is seen in a space filling model of crystal structure 2NMP in **Figure B.3**. Unlike the Di-E-GSSG kinetic results, the addition of the 200 and 300-double mutant rates do not

appear to equal that of the *WT*. This suggests that some of the other 6 free thiols found on CSE play some small role in disulfide bond cleavage.

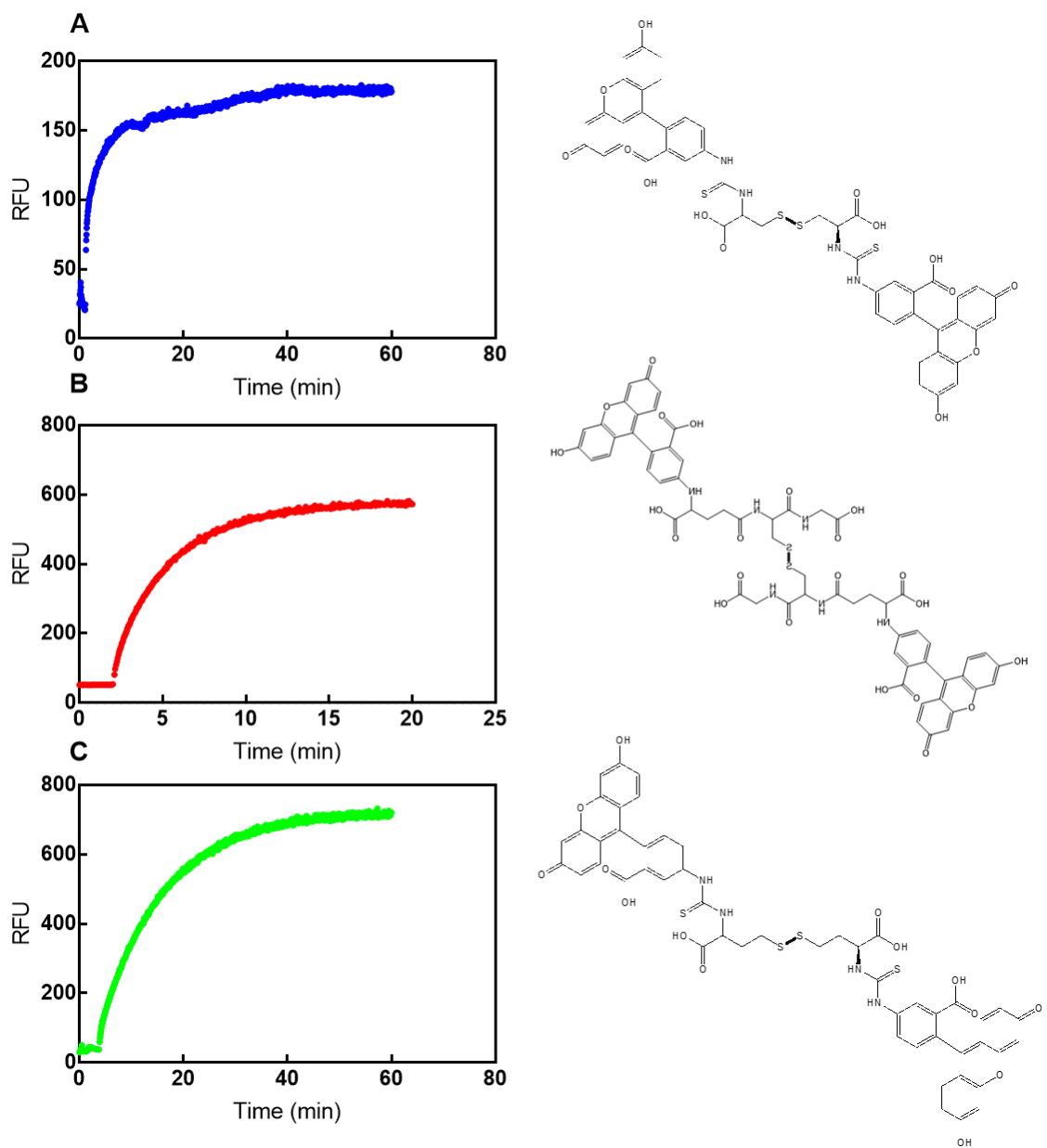


Figure 3.3 (A) 10-Fold fluorescence increase of FITC₂-cystine, as well as proposed structure. (B) 12-fold fluorescence increase of FITC₂-GSSG; proposed structure. (C) 18-fold fluorescence increase of FITC₂-homocystine after reduction by DTT, as well as the proposed structure.

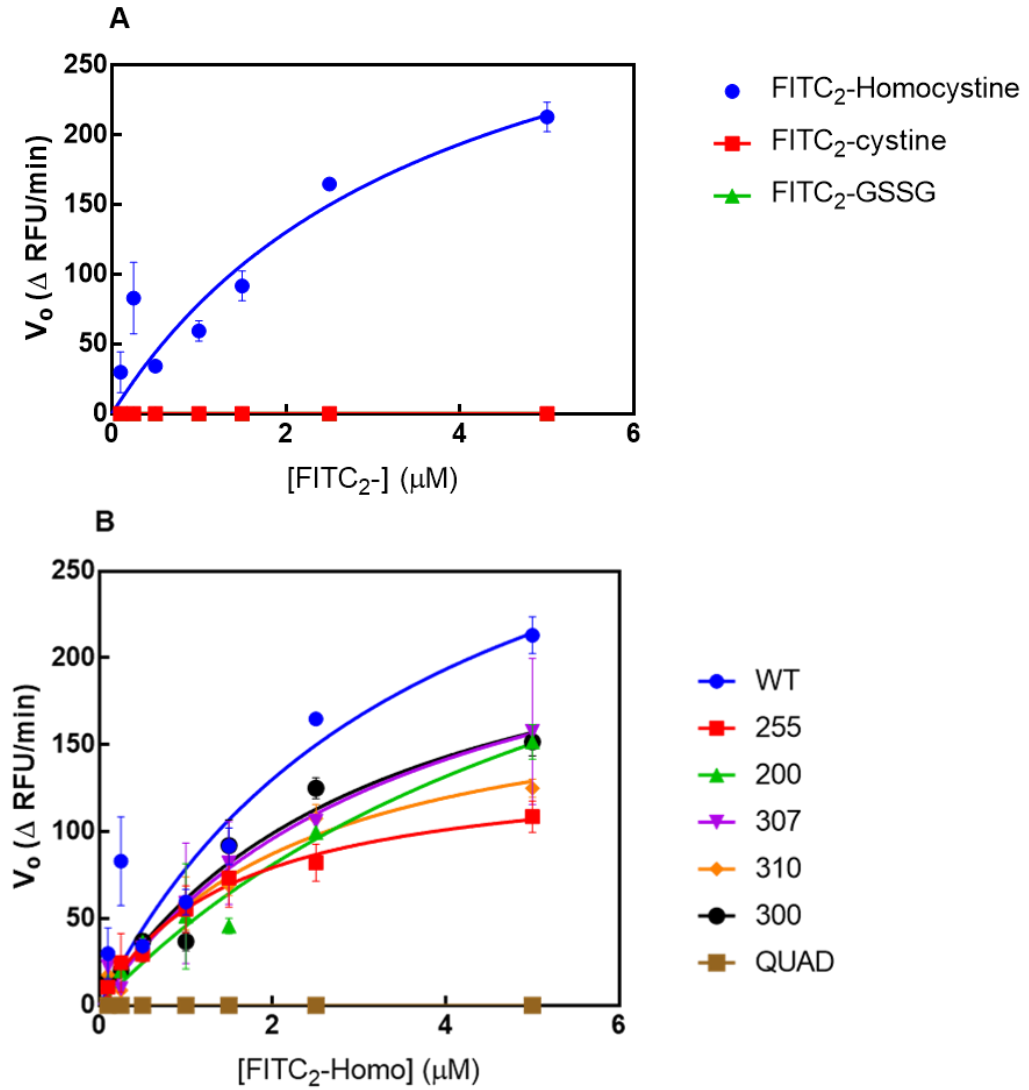


Figure 3.4 Fluorescent free thiol probe kinetics. (A) Testing of the three synthesized fluorescent probes. Only FITC₂-homocystine displays some form of rate with CSE. (B) Testing of FITC₂-homocystine with CSE mutants.

The potential of free thiols influencing the kinetic data was investigated using an SDS-PAGE model and DTNB as a free thiol blocker, which is explored below. As stated in *Section 2.2.7*, two different approaches were utilized in an attempt to quantify the difference in labelling efficiencies of the four free thiol probes. These results are shown in **Figure 3.5**. The effect of DTNB blocking free thiols can be seen in both panels **A** and **B**. Panel **A** shows a representative image of free thiol probe labelling of the *WT* enzyme. The cystine probe shows marginal activity, but the presence of DTNB completely removes the labelling. Likewise, Di-E-GSSG is completely void of any labelling, independent of DTNB. The fluorescence per nanogram of protein indicates efficiency and preference in binding. FITC₂-Homocystine, even with the blocking of free thiols by DTNB shows the highest degree of fluorescent labeling. Both FITC₂-GSSG and Di-E-GSSG shows the lowest labeling efficiency, while FITC₂-cystine shows a marginally increased rate. Interestingly, the C255S mutant shows the highest degree of fluorescence/ng of CSE, more so than that of the *WT*. Unsurprisingly, the quad mutant has the lowest amount of labelling of the mutants tested. The lack of the purported active sites kills any chance of activity. Additionally, all single mutants seem to show a higher degree of labelling over the *WT*, as the single mutants lack that second cysteine which is crucial for the reduction of that intramolecular disulfide formed between the vicinal cysteine and the probe.

A more direct comparison of the fluorescent probes propensity to label each mutant CSE construct can be seen in panel **C** and a graphical comparison of each probes labelling specificity towards each CSE construct which can be seen in **D**. In the representative FITC₂-Homocystine labelled image in **C**, the three single mutants, C255S, C307S, and C310S appear to have a greater amount of FITC₂-Homocystine, and thus show a larger

amount of fluorescence. Of further note is the behavior of the 300 mutants; C307S, and C310S. Both show a higher degree of labelling when compared to the other constructs. The C307-X-X-C310 motif is located on the periphery of the enzyme, and as can be seen in **B.3**, the Cys310 is solvent exposed. This allows for easier access to the reducing free thiol of the mutated enzyme. This phenomenon is not seen in the *WT* as the motif is able to reduce that intramolecular disulfide, kicking off the fluorescent tag.

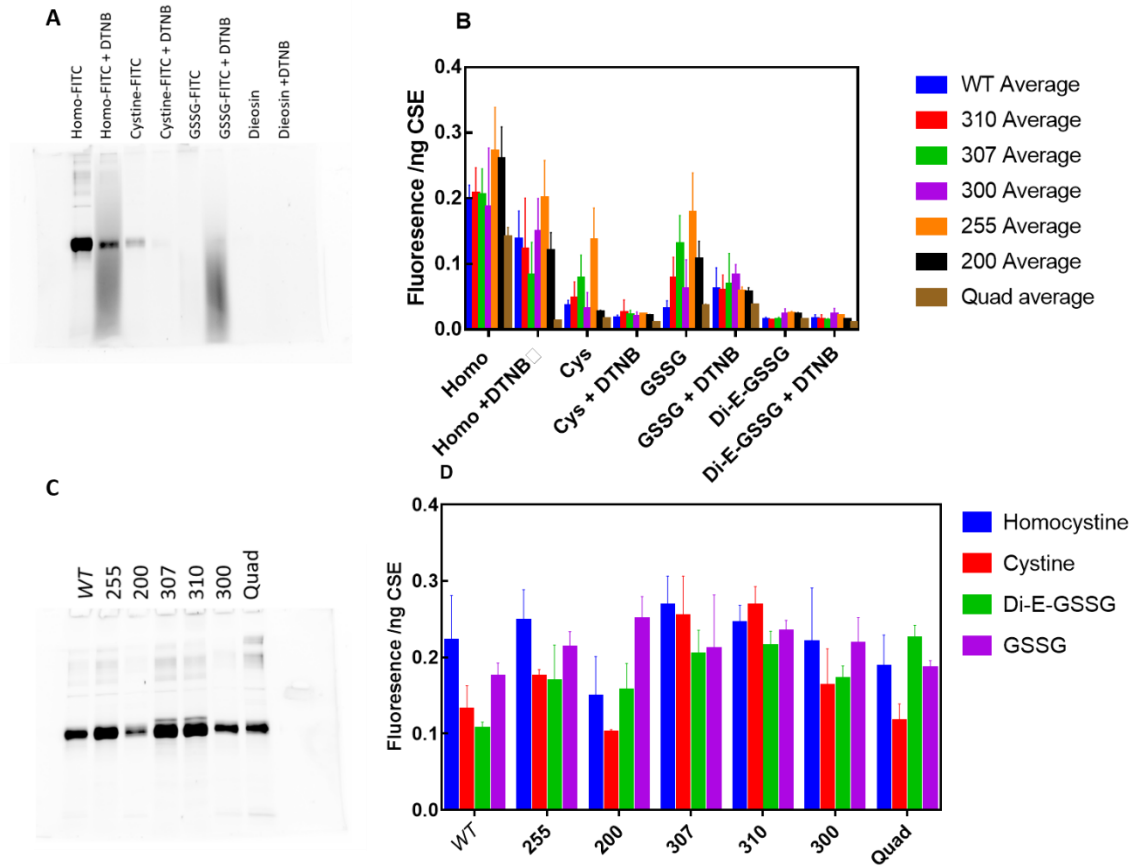


Figure 3.5 Visualization and quantification of fluorescent labelling by free thiol probes. (A) Representative image of WT CSE fluorescently labelled by the four probes. (B) Comparison of both CSE mutant's propensity to become fluorescently labelled as well as the effect of blocking free thiols on fluorescent output. (C) Representative image of FITC₂-Homocysteine labelling of all CSE proteins. (D) Comparison of various probes specificity in labelling CSE mutants.

3.6 Mass Spectrometry

The bulk of the HPLC-ESI MS thus far has given no results. While an 89% sequence coverage of the *WT* protein has been achieved, no direct identification of a successfully modified peptide of interest has been observed thus far. The mass fingerprints of the two peptides of interest, those of the CxxC motifs can be seen in **Figure 3.6**. These peptides have a m/z of 783.345 for the CTGC containing CxxC, and a m/z of 1104.501 for the CYLC containing CxxC. The 783.345 m/z peptide has a charge of +3 and relates to the C₃₀₇-X-X-C₃₁₀ motif. The 1104.501 m/z peptide has a charge of +2 and relates to the more interior C₂₅₂-X-X-C₂₅₅ motif. When either of the C₃₀₇-X-X-C₃₁₀ cysteines are mutated to a serine, the 783 peak is no longer observed, which is to be expected, but the replacement peak is not visible.

The holoenzyme mass spectrometry performed has shown a positive result thus far. As opposed to proteolytic digestion, the monomer was run as a holo-enzyme. **Figure 3.7** shows four mass fingerprints; A is the C307S mutant incubated with homocystine, B is the C310S mutant incubated with homocystine, C is the untreated *WT* enzyme, while D is *WT* incubated with homocystine. Both samples A, and B show an increase in approximately 132 Daltons, which indicates homocystine addition. Sample D shows a peak that is 132 Daltons heavier than that of the untreated *WT* in sample C. In addition, we observe a PTM of some 39 Daltons, which is an unknown entity. While the confirmation of homocystine addition is a result, it is inconclusive as the sample preparation for this mass spectrometry cannot identify the site of modification.

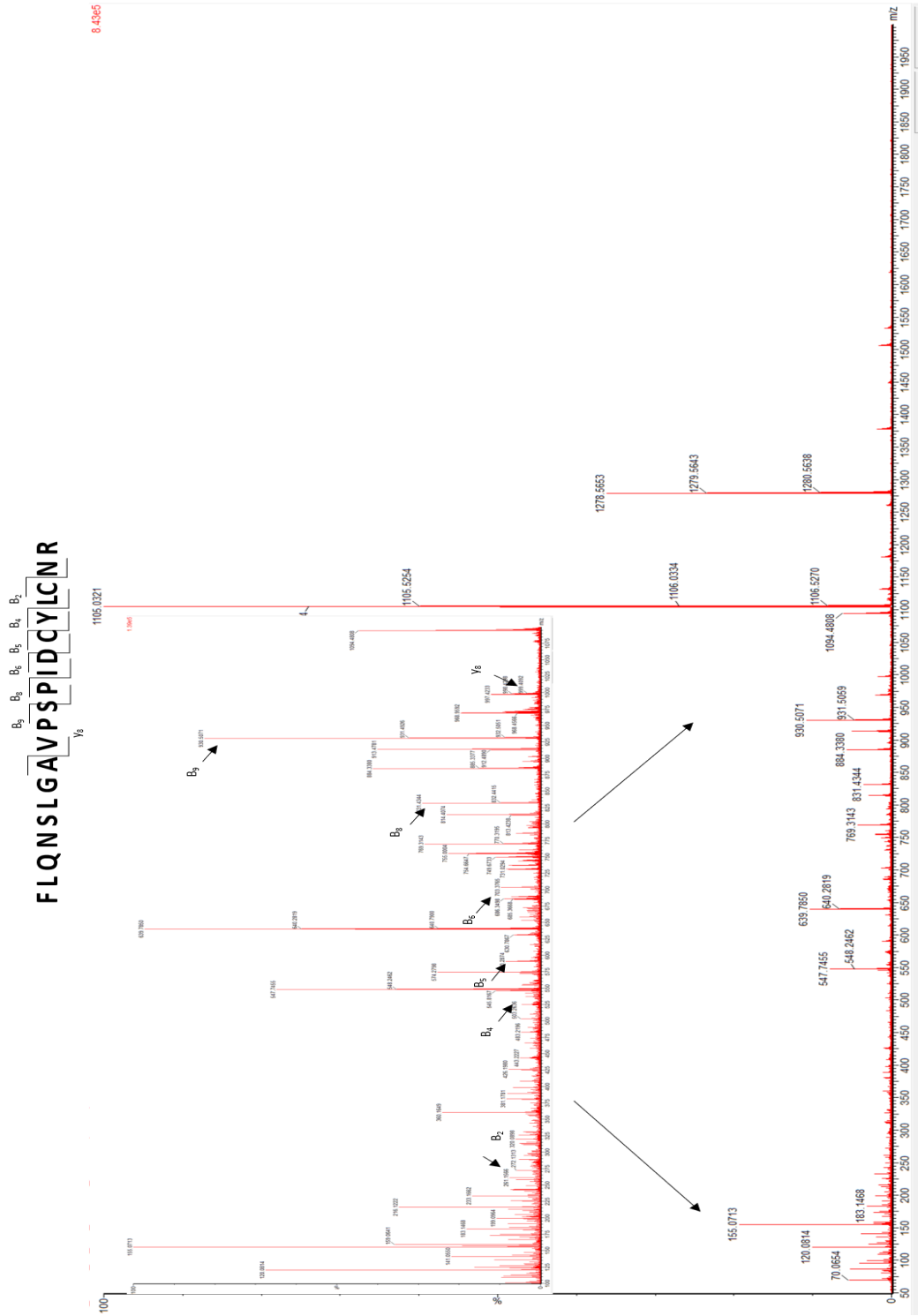
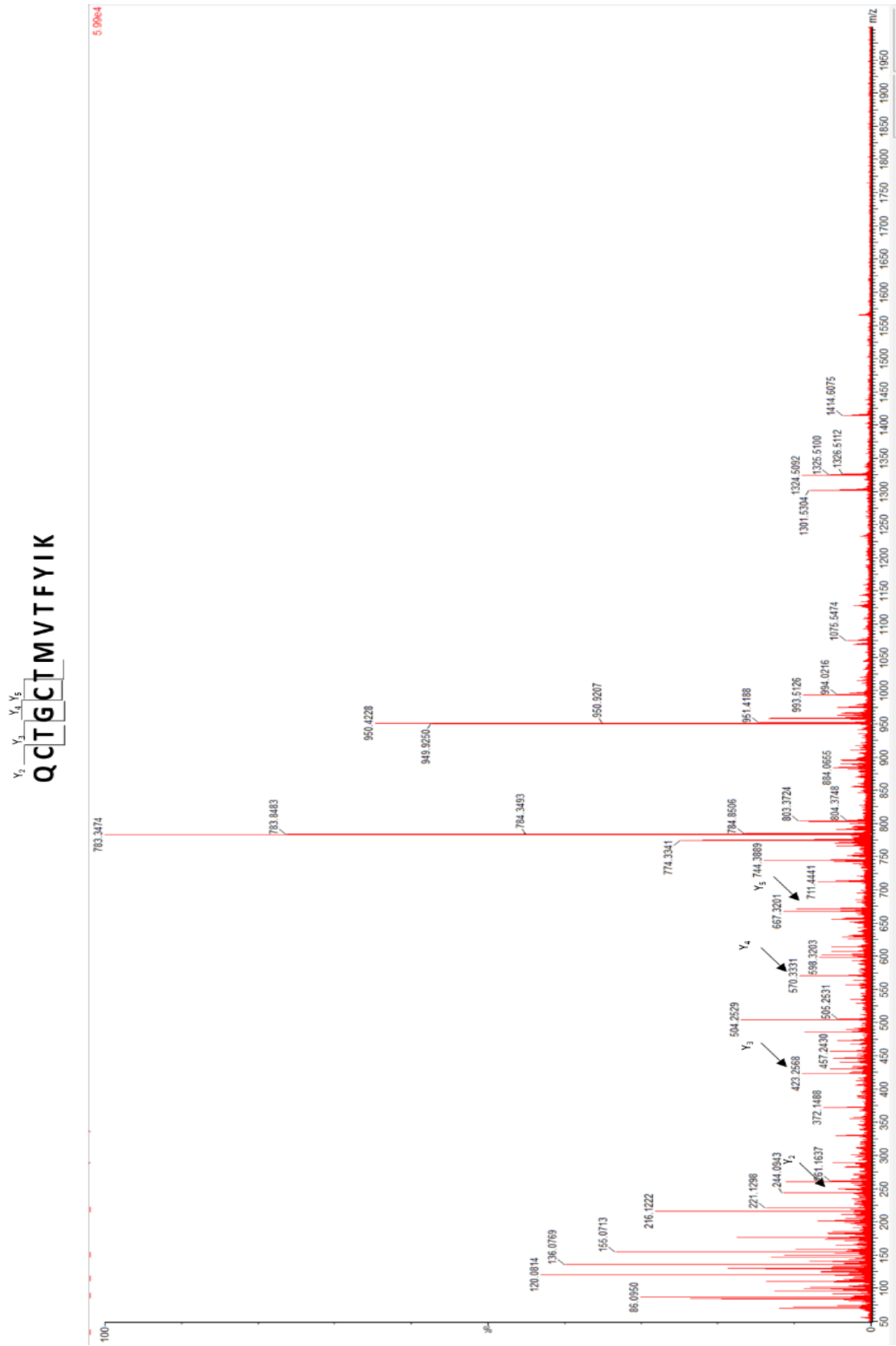


Figure 3.6 (A) CxxC mass spec fingerprints. CYLC fingerprint corresponds to the 200-motif.



(B) CTGC fingerprint corresponds to the 300-motif

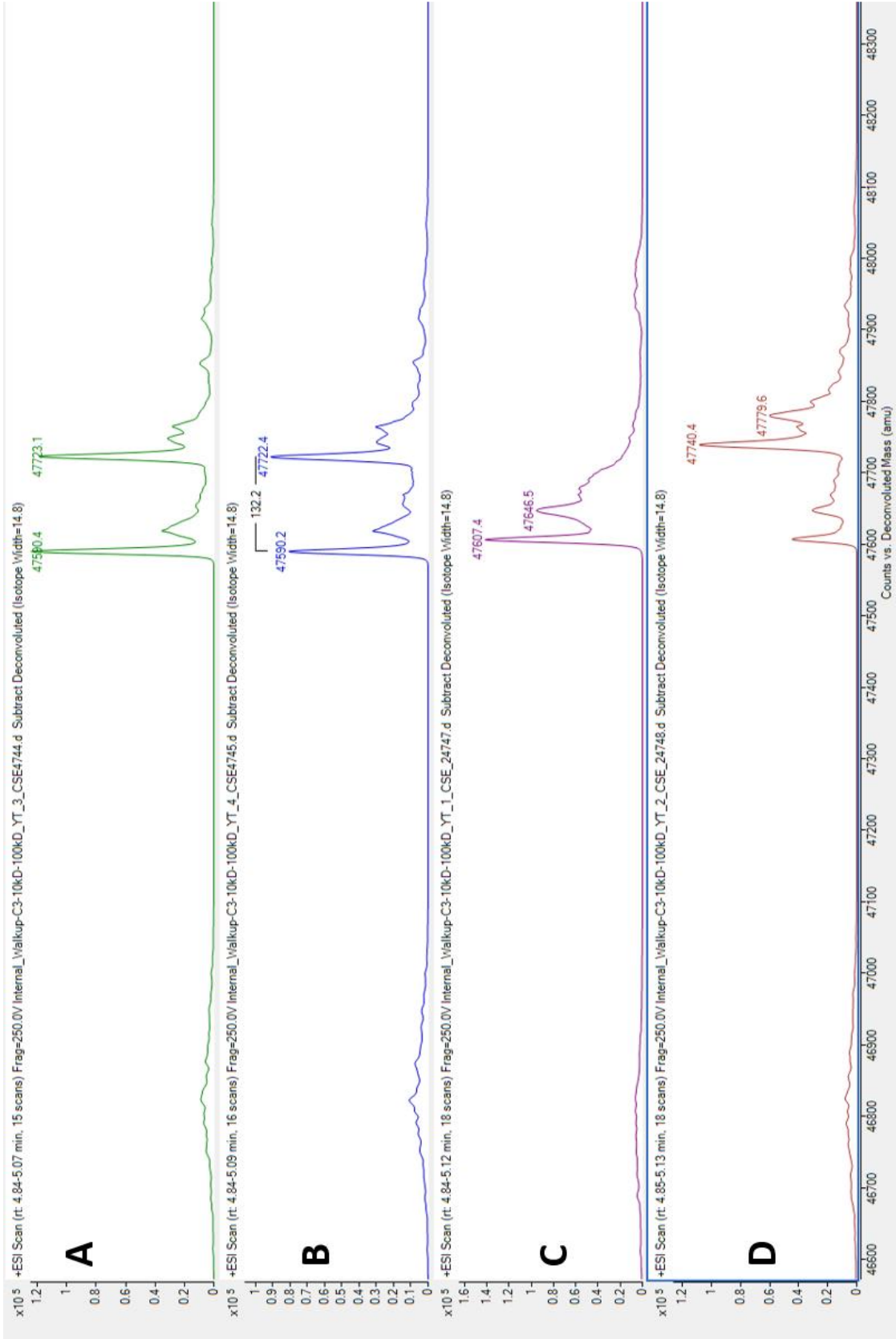


Figure 3.7 Holoenzyme mass spectrometry. (A) C307S, shows an addition of 132.2 Daltons, half homocystine. (B) C310S, shows an addition of 132.2 Daltons, half homocystine. (C) *WT* enzyme, unmodified, with an unknown 39 Dalton modification. (D) Modified *WT*, showing both the half homocystine addition as well as the unknown 39 Dalton modification.

CHAPTER 4:
DISCUSSION

4.1 CSE *In-vitro* Kinetics

The various steady state kinetic assays performed support a crucial role for the hypothesis that the CXXC motifs are involved in regulation of the enzyme, as well as contain a secondary disulfide reducing active site. The catabolism of L-cystathionine is a key indicator of overall enzyme activity. The results show a larger regulatory role for the more interior CXXC motif, the C₂₅₂-X-X-C₂₅₅ motif, specifically the Cys252 residue. This residue appears to be a key residue for the enzyme, as a point mutation results in a lack of cystathionine catabolism. A secondary piece of evidence in support of Cys252 playing an active role in the function of the enzyme is the production and isolation issues that plagued the project. A usable quantity of enzyme was purified only once, with multiple purification attempts resulting in sub-microgram quantities. Cys255 shows a large decrease in activity compared to *WT*, showing 62% of the catalytic activity. This motif is located near the dimer-dimer interface, is located entirely within an alpha-helix, and is almost entirely buried within the enzyme, which gives validity to the hypothesis that this motif is involved in the regulation and function of the enzyme.

While the C₂₅₂-X-X-C₂₅₅ is more involved in enzyme regulation, the C₃₀₇-X-X-C₃₁₀ motif is hypothesized to contain a secondary disulfide reducing active site. The cystathionine catabolism of the single mutants is marginally affected. The double mutant remains catalytically active, with some loss in function; although that is almost certainly a result of steric hindrance interfering with normal enzyme function.

The response of each CSE mutant to a change in pH indicates the optimal pH for maximal enzyme activity. Wildtype CSE was shown to have maximum enzyme activity at a pH of 7.8, which is lower than what has been reported in literature [85]. This raises an

interesting issue as the pH of 8.0 for the standard CSE assay buffers was chosen due its relation to the reported maximum pH of 8.2. As DTNB begins to rapidly degrade in phosphate buffer above pH 8.0, 8.0 was selected for the assay buffer as it was the closest to the reported maximal activity pH without introducing false rates due to the degradation of DTNB. Performing the kinetics again in a lower pH, 7.8, could lead to a more appropriate picture of the enzyme's true activity. Interestingly, C255S shows a max activity at pH 8.2, the only enzyme tested to match what is reported in literature. The C252S, 200-double and quad mutant were not examined due to a lack of activity.

The effects seen by changes in pH on activity of the mutants is quite surprising. With a pI of 6.18, CSE is positively charged in its environment in the cytosol. The mutation of the cysteine residues has no net effect on the pI of the enzyme, so the response to change in pH must be the result of some other changes in the enzyme. As the 300-double mutant displays a pH curve that is mostly flat in nature, as well as the lowest activity of the mutants tested, one can assume that the introduction of the oxygen on serine affects the overall integrity of the local area. This can possibly explain the greater effect observed on the double mutants.

When compared to regulation of its counterpart, cystathionine β -lyase, the overall regulation of CSE is poorly understood [50]. Attempts to influence activity of CSE by oxidation, reduction, and S-nitrosylation by GSSG, GSH and GSNO respectively, yielded no significant difference to the L-cystathionine catabolism activity of CSE. These experiments were performed before the successful mutagenesis and purification of all the single mutants, leaving, at the time the *WT* and the 300-double as the only catalytically active mutants.

4.2 Fluorescent Free Thiol Probes

The Di-E-GSSG kinetic data shown in **Figure B.2** was the first supporting evidence for a secondary active site in the C₃₀₇-X-X-C₃₁₀ C motif. The observed rate was shown to be independent of the traditional active site, with the 300-motif making up the bulk of the activity. This discovery led to the synthesis of three fluorescent probes. Cystine and homocystine were specifically chosen as a starting material for two reasons: i) both cystine and homocystine are disulfide containing molecules, which is essential for fluorescence self-quenching to occur, (ii) both molecules are postulated to be alternative substrates for CSE. Glutathione disulfide was chosen because it interacts with the transsulfuration pathway in addition to its disulfide. While the structures of the probes could not be directly confirmed *via* solution NMR, the observed fold-increase after treatment with DTT indirectly confirms the proposed structures. Several issues contributed to this, notably the inability to produce probe at a concentration suitable for NMR.

Initial testing of the three probes with CSE was the first indication that there may be some form of specificity involved in the CXXC sites. Both FITC₂-Cystine and FITC₂-GSSG displayed no activity in an *in vitro* kinetic assay similar to that of the Di-E-GSSG assay. The full-scale testing of the FITC₂-homocystine probe revealed a few noteworthy items. First, the C₃₀₇-X-X-C₃₁₀ C motif cysteines show the highest rate of activity with respect to the probe, independent of the *WT*. Unlike the phenomenon that was observed with the Di-E-GSSG probe, the additive rates of the both the 200 and 300-doubles do not equal that of the *WT*. This suggests that there is some contribution by free thiols on CSE to the kinetic rates observed.

To correct for this, DTNB was used to block any free thiols prior to fluorescent labelling by the probes. These results were visualized *via* fluorescent imaging of SDS-PAGE. The results shown in **Figure 3.5 B** and **D** are somewhat contradictory. In the thiol blocking experiments, the specificity of the proposed active site is fully supported. The rates at which FITC₂-homocystine label the various CSE enzymes far exceeds that of the other probes. In addition to the specificity for homocystine, the activity of the single mutants, specifically C307S and C310S exceed that of the *WT*. This is an expected result here. The cysteine to serine mutations lack the second cysteine required to cleave the disulfide formed between the probe and enzyme. In the *WT* the CXXC motif functions as it should; the N-terminal cysteine residue attacks the probe, forming a mixed disulfide, where the C-terminal residue is able to attack the newly formed disulfide and release a reduced product, lowering the observed fluorescence. While the mutants are unable to cleave the formed mixed disulfide between the enzyme and probe, there should exist a higher likelihood that there is an interaction between the probe and enzyme in the first place. The CXXC motif can exist in either a reduced or oxidized state; when oxidized there will be no reaction between the probe and the enzyme. The single mutants lack the ability to form a disulfide, and as such can always initiate a nucleophilic attack. The quad mutant fully supports a secondary active site based on the CXXC motifs. With or without the presence of DTNB, there is little to no fluorescent labelling, indicating that free thiols add an insignificant amount to the observed fluorescence.

While the DTNB experiments support some substrate specificity, the visualization of every mutant construct with each probe is not so convincing. There is a lack of significant difference between the fluorescence/ng of protein. However, some broad

trends can be observed. Homocystine appears to be the preferred fluorescent probe, although there is an instance where cystine appears to be favoured over homocystine. Likewise, the previously observed trend that the single mutants show a higher rate of fluorescence uptake appears to hold true. This is especially true when it comes to the C₃₀₇-X-X-C₃₁₀ C motif. This motif is located on the periphery of the enzyme, and its C-terminal cysteine, Cys310 is the lone solvent exposed residue. In addition, the N-terminal cysteine is located at the end of an alpha-helix. Cysteines located at the end of alpha-helices have a much lower p*K*_a when compared to other cysteines. The electrostatics of the helix direct towards the cysteine, lowering that p*K*_a, which results in a better leaving group [95].

4.3 Mass Spectrometry

Mass spectrometry was employed to determine the exact binding site of the fluorescent probes. Thus far, the critical residue has not been observed. A sequence coverage of 90% has been achieved in *WT* CSE thus far, while C307S and C310S have achieved lower rates of coverage, about 75% each. The peptides corresponding to the CxxC motifs have been identified with full confidence. However, modification of these peptides has yet to be observed. Both homocystine and FITC₂-homocystine have been used in attempt to observe a modification. The probable cause of this observation is that the CxxC motifs are functioning as they should, the modification is cleaved before it can be detected by the MS. Another, unlikely possibility is that the modification, in this instance the FITC₂-homocystien probe, is not suitable to fly. Homocystine should be a much better candidate to fly than the probe, but detection has still not been successful.

The use of C307S and C310S led to new obstacles. The mutation of either

cysteine to a serine resulted in the loss of the peptide of interest, as should happen, however the peptide that should replace it, one 16 Daltons less has yet to be detected. This is independent of any attempt at modification with homocystine. The reason for this is currently unknown.

Mass spectrometry on the holoenzyme, that is, the non-digested enzyme provided the only success seen with mass spectrometry. The *WT*, *C307S*, and *C310S* have had an addition of 132.2 Daltons detected. This is consistent with homocystine addition. One can only speculate as to why the modified holoenzyme has been detected and no modified peptide has. There is a possibility that the modification interferes with the active site of trypsin, inhibiting the cleavage around the *CXXC* motifs. The peptides surrounding the *CXXC* were compared to a modified and unmodified sample, and the relative ratios remained unchanged, which does not support the obstruction of trypsin. The formation of dehydroalanine, a modification involving the loss of sulfur on a cysteine residue, which is common in PLP enzyme is also a possibility, as is spontaneous disulfide formation between the tryptic peptides [103].

The use of differential thiol-labelling to map the sites of modification is the next step with mass spectrometry. Any initial modification of a cysteine residue with a probe will protect that residue from modification by a thiol labelling agent, such as *N*-ethylmaleimide. The disulfide can then be reduced and labelled with another labelling agent, such as iodoacetamide, which should allow for easier detection by MS.

4.4 Proposed Mechanism of Action

We propose a novel activity of the *CxxC* sites found in CSE. Of the three fluorogenic probes synthesized, CSE shows a preference to FITC₂-homocystine which

can be explained through the geometry of the disulfide bonds. Energy minimized MM2 structures of the three probes show that homocystine has the smallest disulfide dihedral angle. The cystine probe has a disulfide dihedral of almost 90 °, while the GSSG probe has an angle of 128°. The larger angles prevent interaction with the CxxC sites, as the remainder of the probes cause an increase in steric hindrance. The homocystine probe has a small enough disulfide dihedral angle that the disulfide bond “presents” itself to the CXXC, facilitating an easier interaction.

The specificity for homocystine can be explained by the role of CSE in oxidative stress pathways, as stated above. High levels of homocystine are indicative of high-oxidative stress, which is common in neurodegenerative diseases. The system x_c⁻ cystine/glutamate transporter is associated with the lowering of oxidative stress, by increasing GSH production. Increase in Nrf2 nuclear localization is responsible for a similar mechanism. We propose that the reduction of homocystine to homocysteine by the CXXC motif increases the intracellular pool of homocysteine, which in turn raised cysteine levels and thus levels of GSH in the cell. Additionally, the modification of the CXXC motifs by homocystine provide the possibility of a mechanism to modify the enzymes activity. Homocystine-induced oxidation of the CXXC motifs present on CSE may result in an increase or decrease of CSE activity in response to various stressors in the body.

CHAPTER 5:
CONCLUSION

The addition of H₂S to the list of gasotransmitters by Wang led to an increase of research on the enzymes responsible for its production. However, the lack of information about the regulation of CSE, specifically the CXXC motifs located in CSE is an area of interest. Mutation of key cysteine residues involved in CSE CXXC motifs revealed a key residue, C252S, which when mutated kills all activity. *In vitro* kinetic assays revealed disulfide reductase activity associated with the C₃₀₇-X-X-C₃₁₀ motif. Fluorogenic probes designed to interrogate the function of this motif revealed a specificity to homocystine. Electrospray ionization mass spectrometry was performed with the intent of detecting homocystine addition to a CxxC motif but was unsuccessful. However, homocystine addition to the WT, C307S, and C310S holoenzyme was.

Future directions for this project are twofold. Definitive structures of the probe need to be determined by solution NMR. In addition, mutation of the cysteine residues to a more neutral amino acid, such as alanine could give further insight into the roles of the CXXC motifs. Lastly, successful identification of a modified peptide by mass spectrometry is essential. Differential thiol labelling or switching from ESI-MS to a less energy intensive method such as matrix assisted laser desorption/ionization (MALDI) MS to further increase the chance of detection.

REFERENCES/BIBLIOGRAPHY

- [1] C.W. Scheele, The Stinking Sulfur Air, *Chemical Treatise On Air and Fire* (1777) 149-155.
- [2] J.B. West, Carl Wilhelm Scheele, the discoverer of oxygen, and a very productive chemist, *American journal of physiology. Lung cellular and molecular physiology* 307(11) (2014) L811-6.
- [3] C.R. Hoidal, A.H. Hall, M.D. Robinson, K. Kulig, B.H. Rumack, Hydrogen sulfide poisoning from toxic inhalations of roofing asphalt fumes, *Annals of Emergency Medicine* 15(7) (1986) 826-830.
- [4] S. Monge-Corella, J. García-Pérez, N. Aragonés, M. Pollán, B. Pérez-Gómez, G. López-Abente, Lung cancer mortality in towns near paper, pulp and board industries in Spain: a point source pollution study, *BMC public health* 8 (2008) 288-288.
- [5] M.M. Watt, S.J. Watt, A. Seaton, Episode of toxic gas exposure in sewer workers, *Occupational and environmental medicine* 54(4) (1997) 277-280.
- [6] L.R. Goodwin, D. Francom, F.P. Dieken, J.D. Taylor, M.W. Warencya, R.J. Reiffenstein, G. Dowling, Determination of Sulfide in Brain Tissue by Gas Dialysis/Ion Chromatography: Postmortem Studies and Two Case Reports, *Journal of Analytical Toxicology* 13(2) (1989) 105-109.
- [7] K. Hemminki, M.L. Niemi, COMMUNITY STUDY OF SPONTANEOUS-ABORTIONS - RELATION TO OCCUPATION AND AIR-POLLUTION BY SULFUR-DIOXIDE, HYDROGEN-SULFIDE, AND CARBON-DISULFIDE, *Int. Arch. Occup. Environ. Health* 51(1) (1982) 55-63.
- [8] A.A. Khan, M.M. Schuler, M.G. Prior, S. Yong, R.W. Coppock, L.Z. Florence, L.E. Lillie, Effects of hydrogen sulfide exposure on lung mitochondrial respiratory chain enzymes in rats, *Toxicology and Applied Pharmacology* 103(3) (1990) 482-490.
- [9] D.C. Dorman, F.J.M. Moulin, B.E. McManus, K.C. Mahle, R.A. James, M.F. Struve, Cytochrome Oxidase Inhibition Induced by Acute Hydrogen Sulfide Inhalation: Correlation with Tissue Sulfide Concentrations in the Rat Brain, Liver, Lung, and Nasal Epithelium, *Toxicological Sciences* 65(1) (2002) 18-25.
- [10] C.E. Cooper, G.C. Brown, The inhibition of mitochondrial cytochrome oxidase by the gases carbon monoxide, nitric oxide, hydrogen cyanide and hydrogen sulfide: chemical mechanism and physiological significance, *Journal of Bioenergetics and Biomembranes* 40(5) (2008) 533.
- [11] Y. Li, J.-S. Park, J.-H. Deng, Y. Bai, Cytochrome c oxidase subunit IV is essential for assembly and respiratory function of the enzyme complex, *Journal of bioenergetics and biomembranes* 38(5-6) (2006) 283-291.
- [12] D. Bordo, P. Bork, The rhodanese/Cdc25 phosphatase superfamily. Sequence-structure-function relations, *EMBO reports* 3(8) (2002) 741-6.
- [13] M. Ishigami, K. Hiraki, K. Umemura, Y. Ogasawara, K. Ishii, H. Kimura, A source of hydrogen sulfide and a mechanism of its release in the brain, *Antioxid Redox Signal* 11(2) (2009) 205-14.
- [14] R. Wang, Physiological implications of hydrogen sulfide: a whiff exploration that blossomed, *Physiological reviews* 92(2) (2012) 791-896.

- [15] W. Giggenbach, Optical spectra of highly alkaline sulfide solutions and the second dissociation constant of hydrogen sulfide, *Inorganic Chemistry* 10(7) (1971) 1333-1338.
- [16] R.J. Myers, The new low value for the second dissociation constant for H₂S: Its history, its best value, and its impact on the teaching of sulfide equilibria, *Journal of Chemical Education* 63(8) (1986) 687.
- [17] E. Cuevasanta, A. Denicola, B. Alvarez, M.N. Moller, Solubility and permeation of hydrogen sulfide in lipid membranes, *PloS one* 7(4) (2012) e34562.
- [18] R. Wang, Two's company, three's a crowd: can H₂S be the third endogenous gaseous transmitter?, *FASEB Journal* 16(13) (2002) 1792-1798.
- [19] R. Wang, The gasotransmitter role of hydrogen sulfide, *Antioxid. Redox Signal.* 5(4) (2003) 493-501.
- [20] K. Abe, H. Kimura, The possible role of hydrogen sulfide as an endogenous neuromodulator, *The Journal of Neuroscience* 16(3) (1996) 1066-1071.
- [21] W. Zhao, J. Zhang, Y. Lu, R. Wang, The vasorelaxant effect of H₂S as a novel endogenous gaseous K(ATP) channel opener, *The EMBO journal* 20(21) (2001) 6008-6016.
- [22] W.H. Koppenol, D.M. Stanbury, P.L. Bounds, Electrode potentials of partially reduced oxygen species, from dioxygen to water, *Free Radical Biology and Medicine* 49(3) (2010) 317-322.
- [23] V. Vitvitsky, O. Kabil, R. Banerjee, High turnover rates for hydrogen sulfide allow for rapid regulation of its tissue concentrations, *Antioxid Redox Signal* 17(1) (2012) 22-31.
- [24] Y. Kimura, H. Kimura, Hydrogen sulfide protects neurons from oxidative stress, *FASEB journal : official publication of the Federation of American Societies for Experimental Biology* 18(10) (2004) 1165-7.
- [25] R.J. Bridges, N.R. Natale, S.A. Patel, System xc⁻ cystine/glutamate antiporter: an update on molecular pharmacology and roles within the CNS, *British journal of pharmacology* 165(1) (2012) 20-34.
- [26] Y. Kimura, Y. Goto, H. Kimura, Hydrogen sulfide increases glutathione production and suppresses oxidative stress in mitochondria, *Antioxid Redox Signal* 12(1) (2010) 1-13.
- [27] R. Venè, P. Castellani, L. Delfino, M. Lucibello, M.R. Ciriolo, A. Rubartelli, The Cystine/Cysteine Cycle and GSH Are Independent and Crucial Antioxidant Systems in Malignant Melanoma Cells and Represent Druggable Targets, *Antioxid. Redox Signal.* 15(9) (2011) 2439-2453.
- [28] Z.-Z. Xie, Y. Liu, J.-S. Bian, Hydrogen Sulfide and Cellular Redox Homeostasis, *Oxidative Medicine and Cellular Longevity* 2016 (2016) 12.
- [29] R. Hosoki, N. Matsuki, H. Kimura, The Possible Role of Hydrogen Sulfide as an Endogenous Smooth Muscle Relaxant in Synergy with Nitric Oxide, *Biochemical and Biophysical Research Communications* 237(3) (1997) 527-531.
- [30] W. Zhao, R. Wang, H₂S-induced vasorelaxation and underlying cellular and molecular mechanisms, *American Journal of Physiology-Heart and Circulatory Physiology* 283(2) (2002) H474-H480.
- [31] J.W. Elrod, J.W. Calvert, J. Morrison, J.E. Doeller, D.W. Kraus, L. Tao, X. Jiao, R. Scalia, L. Kiss, C. Szabo, H. Kimura, C.W. Chow, D.J. Lefer, Hydrogen sulfide attenuates myocardial ischemia-reperfusion injury by preservation of mitochondrial

- function, *Proceedings of the National Academy of Sciences of the United States of America* 104(39) (2007) 15560-5.
- [32] Y.Z. Zhu, Z.J. Wang, P. Ho, Y.Y. Loke, Y.C. Zhu, S.H. Huang, C.S. Tan, M. Whiteman, J. Lu, P.K. Moore, Hydrogen sulfide and its possible roles in myocardial ischemia in experimental rats, *Journal of applied physiology* (Bethesda, Md. : 1985) 102(1) (2007) 261-8.
- [33] G. Yang, L. Wu, B. Jiang, W. Yang, J. Qi, K. Cao, Q. Meng, A.K. Mustafa, W. Mu, S. Zhang, S.H. Snyder, R. Wang, H₂S as a physiologic vasorelaxant: hypertension in mice with deletion of cystathionine gamma-lyase, *Science* 322(5901) (2008) 587-90.
- [34] D.J. Elsey, R.C. Fowkes, G.F. Baxter, Regulation of cardiovascular cell function by hydrogen sulfide (H₂S), *Cell biochemistry and function* 28(2) (2010) 95-106.
- [35] B.L. Predmore, D.J. Lefer, Development of hydrogen sulfide-based therapeutics for cardiovascular disease, *Journal of cardiovascular translational research* 3(5) (2010) 487-98.
- [36] K. Kondo, S. Bhushan, A.L. King, S.D. Prabhu, T. Hamid, S. Koenig, T. Murohara, B.L. Predmore, G. Gojon, Sr., G. Gojon, Jr., R. Wang, N. Karusula, C.K. Nicholson, J.W. Calvert, D.J. Lefer, H₂S protects against pressure overload-induced heart failure via upregulation of endothelial nitric oxide synthase, *Circulation* 127(10) (2013) 1116-27.
- [37] S. Mani, H. Li, A. Untereiner, L. Wu, G. Yang, R.C. Austin, J.G. Dickhout, S. Lhotak, Q.H. Meng, R. Wang, Decreased endogenous production of hydrogen sulfide accelerates atherosclerosis, *Circulation* 127(25) (2013) 2523-34.
- [38] Y. Wang, X. Zhao, H. Jin, H. Wei, W. Li, D. Bu, X. Tang, Y. Ren, C. Tang, J. Du, Role of hydrogen sulfide in the development of atherosclerotic lesions in apolipoprotein E knockout mice, *Arteriosclerosis, thrombosis, and vascular biology* 29(2) (2009) 173-9.
- [39] L. Xie, Y. Gu, M. Wen, S. Zhao, W. Wang, Y. Ma, G. Meng, Y. Han, Y. Wang, G. Liu, P.K. Moore, X. Wang, H. Wang, Z. Zhang, Y. Yu, A. Ferro, Z. Huang, Y. Ji, Hydrogen Sulfide Induces Keap1 S-sulfhydration and Suppresses Diabetes-Accelerated Atherosclerosis via Nrf2 Activation, *Diabetes* 65(10) (2016) 3171-84.
- [40] J.W. Calvert, S. Jha, S. Gundewar, J.W. Elrod, A. Ramachandran, C.B. Pattillo, C.G. Kevil, D.J. Lefer, Hydrogen sulfide mediates cardioprotection through Nrf2 signaling, *Circulation research* 105(4) (2009) 365-74.
- [41] Q. Ma, Role of nrf2 in oxidative stress and toxicity, *Annual review of pharmacology and toxicology* 53 (2013) 401-426.
- [42] H. Kimura, Hydrogen sulfide induces cyclic AMP and modulates the NMDA receptor, *Biochem Biophys Res Commun* 267(1) (2000) 129-33.
- [43] Y. Nagai, M. Tsugane, J. Oka, H. Kimura, Hydrogen sulfide induces calcium waves in astrocytes, *FASEB journal : official publication of the Federation of American Societies for Experimental Biology* 18(3) (2004) 557-9.
- [44] L.-F. Hu, Y. Li, K.L. Neo, Q.C. Yong, S.W. Lee, B.K.H. Tan, J.-S. Bian, Hydrogen Sulfide Regulates Na⁺/H⁺ Exchanger Activity via Stimulation of Phosphoinositide 3-Kinase/Akt and Protein Kinase G Pathways, *Journal of Pharmacology and Experimental Therapeutics* 339(2) (2011) 726-735.
- [45] K. Eto, T. Asada, K. Arima, T. Makifuchi, H. Kimura, Brain hydrogen sulfide is severely decreased in Alzheimer's disease, *Biochem Biophys Res Commun* 293(5) (2002) 1485-8.

- [46] B.D. Paul, J.I. Sbdio, R. Xu, M.S. Vandiver, J.Y. Cha, A.M. Snowman, S.H. Snyder, Cystathionine gamma-lyase deficiency mediates neurodegeneration in Huntington's disease, *Nature* 509(7498) (2014) 96-100.
- [47] H. Zhang, Y. Gao, F. Zhao, Z. Dai, T. Meng, S. Tu, Y. Yan, Hydrogen sulfide reduces mRNA and protein levels of beta-site amyloid precursor protein cleaving enzyme 1 in PC12 cells, *Neurochemistry international* 58(2) (2011) 169-75.
- [48] B.V. Nagpure, J.-S. Bian, Hydrogen Sulfide Inhibits A2A Adenosine Receptor Agonist Induced β -Amyloid Production in SH-SY5Y Neuroblastoma Cells via a cAMP Dependent Pathway, *PloS one* 9(2) (2014) e88508.
- [49] J.I. Sbdio, S.H. Snyder, B.D. Paul, Transcriptional control of amino acid homeostasis is disrupted in Huntington's disease, *Proceedings of the National Academy of Sciences of the United States of America* 113(31) (2016) 8843-8.
- [50] M.R. Filipovic, J. Zivanovic, B. Alvarez, R. Banerjee, Chemical Biology of H₂S Signaling through Persulfidation, *Chemical Reviews* 118(3) (2018) 1253-1337.
- [51] M. Bhatia, H₂S and Inflammation: An Overview, *Handbook of experimental pharmacology* 230 (2015) 165-80.
- [52] Y. Hui, J. Du, C. Tang, G. Bin, H. Jiang, Changes in arterial hydrogen sulfide (H₂S) content during septic shock and endotoxin shock in rats, *Journal of Infection* 47(2) (2003) 155-160.
- [53] M. Whiteman, L. Li, P. Rose, C.-H. Tan, D.B. Parkinson, P.K. Moore, The effect of hydrogen sulfide donors on lipopolysaccharide-induced formation of inflammatory mediators in macrophages, *Antioxid. Redox Signal.* 12(10) (2010) 1147-1154.
- [54] J. Loubinoux, J.P. Bronowicki, I.A. Pereira, J.L. Mougengel, A.E. Faou, Sulfate-reducing bacteria in human feces and their association with inflammatory bowel diseases, *FEMS microbiology ecology* 40(2) (2002) 107-12.
- [55] S. Fiorucci, E. Antonelli, A. Mencarelli, S. Orlandi, B. Renga, G. Rizzo, E. Distrutti, V. Shah, A. Morelli, The third gas: H₂S regulates perfusion pressure in both the isolated and perfused normal rat liver and in cirrhosis, *Hepatology (Baltimore, Md.)* 42(3) (2005) 539-48.
- [56] B. Srilatha, P.G. Adaikan, P.K. Moore, Possible role for the novel gasotransmitter hydrogen sulphide in erectile dysfunction--a pilot study, *European journal of pharmacology* 535(1-3) (2006) 280-2.
- [57] L.P. Fang, Q. Lin, C.S. Tang, X.M. Liu, Hydrogen sulfide suppresses migration, proliferation and myofibroblast transdifferentiation of human lung fibroblasts, *Pulmonary pharmacology & therapeutics* 22(6) (2009) 554-61.
- [58] M.M. Perry, C.K. Hui, M. Whiteman, M.E. Wood, I. Adcock, P. Kirkham, C. Michaeloudes, K.F. Chung, Hydrogen sulfide inhibits proliferation and release of IL-8 from human airway smooth muscle cells, *American journal of respiratory cell and molecular biology* 45(4) (2011) 746-52.
- [59] X. Qiu, J. Villalta, G. Lin, T.F. Lue, Role of hydrogen sulfide in the physiology of penile erection, *Journal of andrology* 33(4) (2012) 529-535.
- [60] H. Li, S.-J. Feng, G.-Z. Zhang, S.-X. Wang, Correlation of lower concentrations of hydrogen sulfide with atherosclerosis in chronic hemodialysis patients with diabetic nephropathy, *Blood Purif* 38(3-4) (2014) 188-194.
- [61] E. Blackstone, M. Morrison, M.B. Roth, H₂S induces a suspended animation-like state in mice, *Science* 308(5721) (2005) 518.

- [62] C. Szabo, C. Ransy, K. Modis, M. Andriamihaja, B. Murgheș, C. Coletta, G. Olah, K. Yanagi, F. Bouillaud, Regulation of mitochondrial bioenergetic function by hydrogen sulfide. Part I. Biochemical and physiological mechanisms, *Br J Pharmacol* 171(8) (2014) 2099-122.
- [63] E. Cuevasanta, M. Lange, J. Bonanata, E.L. Coitiño, G. Ferrer-Sueta, M.R. Filipovic, B. Alvarez, Reaction of Hydrogen Sulfide with Disulfide and Sulfenic Acid to Form the Strongly Nucleophilic Persulfide, *The Journal of biological chemistry* 290(45) (2015) 26866-26880.
- [64] P.K. Yadav, M. Martinov, V. Vitvitsky, J. Seravalli, R. Wedmann, M.R. Filipovic, R. Banerjee, Biosynthesis and Reactivity of Cysteine Persulfides in Signaling, *Journal of the American Chemical Society* 138(1) (2016) 289-99.
- [65] T. Ida, T. Sawa, H. Ihara, Y. Tsuchiya, Y. Watanabe, Y. Kumagai, M. Suematsu, H. Motohashi, S. Fujii, T. Matsunaga, M. Yamamoto, K. Ono, N.O. Devarie-Baez, M. Xian, J.M. Fukuto, T. Akaike, Reactive cysteine persulfides and S-polythiolation regulate oxidative stress and redox signaling, *Proceedings of the National Academy of Sciences of the United States of America* 111(21) (2014) 7606-11.
- [66] M. Libiad, P.K. Yadav, V. Vitvitsky, M. Martinov, R. Banerjee, Organization of the human mitochondrial hydrogen sulfide oxidation pathway, *J Biol Chem* 289(45) (2014) 30901-10.
- [67] A.K. Mustafa, G. Sikka, S.K. Gazi, J. Steppan, S.M. Jung, A.K. Bhunia, V.M. Barodka, F.K. Gazi, R.K. Barrow, R. Wang, L.M. Amzel, D.E. Berkowitz, S.H. Snyder, Hydrogen sulfide as endothelium-derived hyperpolarizing factor sulfhydrates potassium channels, *Circulation research* 109(11) (2011) 1259-68.
- [68] N. Krishnan, C. Fu, D.J. Pappin, N.K. Tonks, H₂S-Induced sulfhydration of the phosphatase PTP1B and its role in the endoplasmic reticulum stress response, *Science signaling* 4(203) (2011) ra86.
- [69] J.W. Kaspar, S.K. Niture, A.K. Jaiswal, Nrf2:INrf2 (Keap1) signaling in oxidative stress, *Free radical biology & medicine* 47(9) (2009) 1304-9.
- [70] N. Wakabayashi, A.T. Dinkova-Kostova, W.D. Holtzclaw, M.I. Kang, A. Kobayashi, M. Yamamoto, T.W. Kensler, P. Talalay, Protection against electrophile and oxidant stress by induction of the phase 2 response: fate of cysteines of the Keap1 sensor modified by inducers, *Proceedings of the National Academy of Sciences of the United States of America* 101(7) (2004) 2040-5.
- [71] E. Fischer, Bildung von Methylenblau als Reaktion auf Schwefelwasserstoff, *European Journal of Inorganic Chemistry* 16(2) (1883) 1521-3140.
- [72] J.K. Fogo, M. Popowsky, Spectrophotometric Determination of Hydrogen Sulfide, *Analytical Chemistry* 21(6) (1949) 732-734.
- [73] M.N. Hughes, M.N. Centelles, K.P. Moore, Making and working with hydrogen sulfide: The chemistry and generation of hydrogen sulfide in vitro and its measurement in vivo: a review, *Free radical biology & medicine* 47(10) (2009) 1346-53.
- [74] N.L. Whitfield, E.L. Kreimler, F.C. Verdial, N. Skovgaard, K.R. Olson, Reappraisal of H₂S/sulfide concentration in vertebrate blood and its potential significance in ischemic preconditioning and vascular signaling, *American journal of physiology. Regulatory, integrative and comparative physiology* 294(6) (2008) R1930-7.
- [75] K.R. Olson, A practical look at the chemistry and biology of hydrogen sulfide, *Antioxid. Redox Signal.* 17(1) (2012) 32-44.

- [76] E.A. Wintner, T.L. Deckwerth, W. Langston, A. Bengtsson, D. Leviten, P. Hill, M.A. Insko, R. Dumpit, E. VandenEkar, C.F. Toombs, C. Szabo, A monobromobimane-based assay to measure the pharmacokinetic profile of reactive sulphide species in blood, *Br J Pharmacol* 160(4) (2010) 941-57.
- [77] P. Jeroschewski, C. Steuckart, M. Köhl, An Amperometric Microsensor for the Determination of H₂S in Aquatic Environments, *Analytical Chemistry* 68(24) (1996) 4351-4357.
- [78] T. Ubuka, Assay methods and biological roles of labile sulfur in animal tissues, *Journal of chromatography. B, Analytical technologies in the biomedical and life sciences* 781(1-2) (2002) 227-49.
- [79] M.H. Stipanuk, SULFUR AMINO ACID METABOLISM: Pathways for Production and Removal of Homocysteine and Cysteine, *Annual Review of Nutrition* 24(1) (2004) 539-577.
- [80] M.H. Stipanuk, P.W. Beck, Characterization of the enzymic capacity for cysteine desulphhydration in liver and kidney of the rat, *Biochemical Journal* 206(2) (1982) 267-277.
- [81] Y. Ogasawara, S. Isoda, S. Tanabe, Tissue and subcellular distribution of bound and acid-labile sulfur, and the enzymic capacity for sulfide production in the rat, *Biological & pharmaceutical bulletin* 17(12) (1994) 1535-42.
- [82] H. Teng, B. Wu, K. Zhao, G. Yang, L. Wu, R. Wang, Oxygen-sensitive mitochondrial accumulation of cystathionine β -synthase mediated by Lon protease, *Proceedings of the National Academy of Sciences of the United States of America* 110(31) (2013) 12679-12684.
- [83] O. Kabil, Y. Zhou, R. Banerjee, Human Cystathionine β -Synthase Is a Target for Sumoylation, *Biochemistry* 45(45) (2006) 13528-13536.
- [84] R.V. Banerjee, R.G. Matthews, Cobalamin-dependent methionine synthase, *FASEB journal : official publication of the Federation of American Societies for Experimental Biology* 4(5) (1990) 1450-9.
- [85] C. Steegborn, T. Clausen, P. Sondermann, U. Jacob, M. Worbs, S. Marinkovic, R. Huber, M.C. Wahl, Kinetics and inhibition of recombinant human cystathionine gamma-lyase. Toward the rational control of transsulfuration, *J Biol Chem* 274(18) (1999) 12675-84.
- [86] Y. Mikami, N. Shibuya, Y. Kimura, N. Nagahara, Y. Ogasawara, H. Kimura, Thioredoxin and dihydrolipoic acid are required for 3-mercaptopyruvate sulfurtransferase to produce hydrogen sulfide, *The Biochemical journal* 439(3) (2011) 479-85.
- [87] A.L. Levonen, R. Lapatto, M. Saksela, K.O. Raivio, Human cystathionine gamma-lyase: developmental and in vitro expression of two isoforms, *The Biochemical journal* 347 Pt 1 (2000) 291-5.
- [88] G. Yang, X. Sun, R. Wang, Hydrogen sulfide-induced apoptosis of human aorta smooth muscle cells via the activation of mitogen-activated protein kinases and caspase-3, *FASEB journal : official publication of the Federation of American Societies for Experimental Biology* 18(14) (2004) 1782-4.
- [89] Q. Sun, R. Collins, S. Huang, L. Holmberg-Schiavone, G.S. Anand, C.H. Tan, S. van-den-Berg, L.W. Deng, P.K. Moore, T. Karlberg, J. Sivaraman, Structural basis for the inhibition mechanism of human cystathionine gamma-lyase, an enzyme responsible for the production of H₂S, *J Biol Chem* 284(5) (2009) 3076-85.

- [90] M. Whiteman, S. Le Trionnaire, M. Chopra, B. Fox, J. Whatmore, Emerging role of hydrogen sulfide in health and disease: critical appraisal of biomarkers and pharmacological tools, *Clinical science (London, England : 1979)* 121(11) (2011) 459-88.
- [91] G. Yuan, C. Vasavda, Y.J. Peng, V.V. Makarenko, G. Raghuraman, J. Nanduri, M.M. Gadalla, G.L. Semenza, G.K. Kumar, S.H. Snyder, N.R. Prabhakar, Protein kinase G-regulated production of H₂S governs oxygen sensing, *Science signaling* 8(373) (2015) ra37.
- [92] C. Frauer, A. Rottach, D. Meilinger, S. Bultmann, K. Fellingner, S. Hasenoder, M. Wang, W. Qin, J. Soding, F. Spada, H. Leonhardt, Different binding properties and function of CXXC zinc finger domains in Dnmt1 and Tet1, *PloS one* 6(2) (2011) e16627.
- [93] R. Noiva, Protein disulfide isomerase: the multifunctional redox chaperone of the endoplasmic reticulum, *Seminars in cell & developmental biology* 10(5) (1999) 481-93.
- [94] D.E. Fomenko, V.N. Gladyshev, Identity and Functions of CxxC-Derived Motifs, *Biochemistry* 42(38) (2003) 11214-11225.
- [95] T. Kortemme, T.E. Creighton, Ionisation of cysteine residues at the termini of model alpha-helical peptides. Relevance to unusual thiol pK_a values in proteins of the thioredoxin family, *Journal of molecular biology* 253(5) (1995) 799-812.
- [96] A. Raturi, Panayiotis O. Vacratsis, D. Seslija, L. Lee, B. Mutus, A direct, continuous, sensitive assay for protein disulphide-isomerase based on fluorescence self-quenching, *Biochemical Journal* 391(2) (2005) 351-357.
- [97] L.J. Jones, R.H. Upson, R.P. Haugland, N. Panchuk-Voloshina, M. Zhou, R.P. Haugland, Quenched BODIPY dye-labeled casein substrates for the assay of protease activity by direct fluorescence measurement, *Analytical biochemistry* 251(2) (1997) 144-52.
- [98] P.K. Smith, R.I. Krohn, G.T. Hermanson, A.K. Mallia, F.H. Gartner, M.D. Provenzano, E.K. Fujimoto, N.M. Goeke, B.J. Olson, D.C. Klenk, Measurement of protein using bicinchoninic acid, *Analytical biochemistry* 150(1) (1985) 76-85.
- [99] H.B. Collier, NOTE ON MOLAR ABSORPTIVITY OF REDUCED ELLMANS REAGENT, 3-CARBOXYLATO-4-NITROTHIOPHENOLATE, *Analytical biochemistry* 56(1) (1973) 310-311.
- [100] G.L. Ellman, Tissue sulfhydryl groups, *Archives of Biochemistry and Biophysics* 82(1) (1959) 70-77.
- [101] A. Asimakopoulou, P. Panopoulos, C.T. Chasapis, C. Coletta, Z. Zhou, G. Cirino, A. Giannis, C. Szabo, G.A. Spyroulias, A. Papapetropoulos, Selectivity of commonly used pharmacological inhibitors for cystathionine beta synthase (CBS) and cystathionine gamma lyase (CSE), *Br J Pharmacol* 169(4) (2013) 922-32.
- [102] A. Shevchenko, H. Tomas, J. Havli, J.V. Olsen, M. Mann, In-gel digestion for mass spectrometric characterization of proteins and proteomes, *Nature Protocols* 1 (2007) 2856.
- [103] R. Bar-Or, L.T. Rael, D. Bar-Or, Dehydroalanine derived from cysteine is a common post-translational modification in human serum albumin, *Rapid communications in mass spectrometry : RCM* 22(5) (2008) 711-6.

APPENDICES

Appendix A (Chapters 1 & 2 supplementary material)

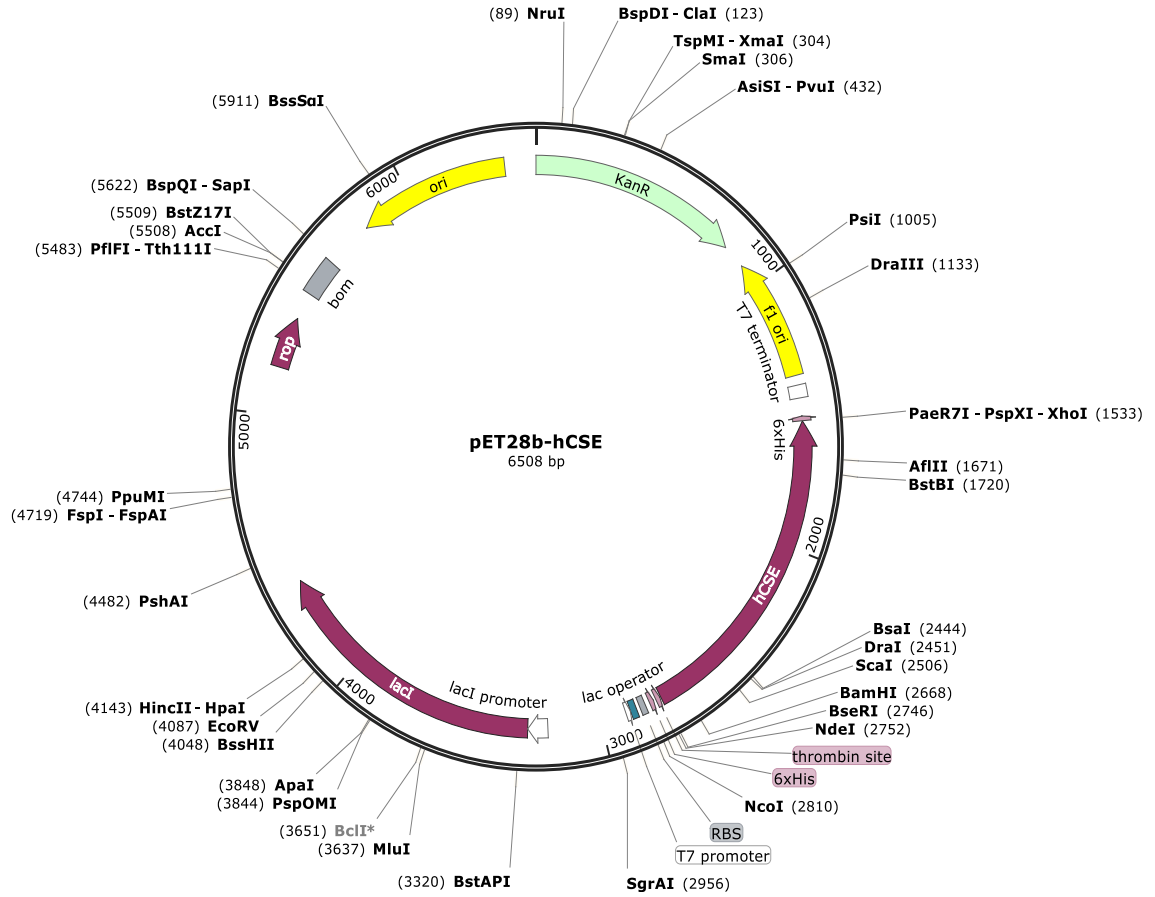


Figure A.1 Plasmid map containing hCSE. CSE plasmid was provided by Dr. Ruma Banerjee of the University of Michigan and the plasmid was cloned into the pET28b-hCSE vector by Dr. Sirinart Ananvoranich of the University of Windsor.

SMQEKDASSQ GFLPHFQHFA TQAIHVGQDP EQWTSRAVVP
PISLSTTFKQ GAPGQHSGFE YSRSGNPTRN CLEKAVAALDG
AKYCLAFASG LAATVTITHL LKAGDQIICM DDVYGGTNRV
FRQVASEFGL KISFVDCSKI KLEAAITPE TKLVWIETPT NPTQKVIDIE
GCAHIVHKHG DIILVVDNTF MSPYFQRPLA LGADISMYS
TKYMNGHSDV VMGLVSVNCE SLHNRLRFLQ NSLGAVPSPI
DCYLCNRGLKT LHVRMEKHFK NGMAVAQFLE SNPWVEKVIY
PGLPSHPQHE LVKRQCTGCT GMVTFYIKGT LQHAEIFLKN
LKLFTLAESLG GFESLAELPA IMTHASVLKN DRDVLGISDT
LIRLSVGLED EEDLLEDLDQA LKAAHPPSGH HHHHH

Figure A.2 hCSE sequence. CxxC residues are bolded and underlined.

Table A.1 Table of PCR Primers used. Changed base pairs are underlined and bolded. For quad mutation, both double primers were used sequentially, mutating one CxxC at a time.

Primer	Sequence (5`-3`)	MT °C
CSE C307S	CTG TAC AAC CTG TAG ACT GAC GCT TCA CC	55
CSE C307S rev	GGA TGG TCA CCT TTT ATA TTA AGG GCA CTC	55
CSE C310S	GAC CAT CCC TGT AGA ACC TGT ACA CTG A	54
CSE C310S rev	ACC TTT TAT ATT AAG GGC ACT CTT CAG CAT G	54
CSE C307S_C310S	CAT CCC TGT AGA ACC TGT AGA CTG ACG CTT CAC	58
CSE C307S_C310S rev	GTC ACC TTT TAT ATT AAG GGC ACT CTT CAG C	58
CSE C252S	CGA TTG CAG AGG TAA GAA TCA ATA GGA GAT GG	56
CSE C252S rev	GGT CTG AAG ACT CTA CAT GTC CGA AT	56
CSE C255S	TCA GAC CTC GAT TGG AGA GGT AAC AAT C	59
CSE C255S rev	GGT CTG AAG ACT CTA CAT GTC CGA AT	59
CSE C252S_C255S	CAG ACC TCG ATT GGA GAG GTA AGA ATC AAT AGG AGA TG	55
CSE C252S_C255S rev	AAG ACT CTA CAT GTC CGA ATG GAA AAG	55

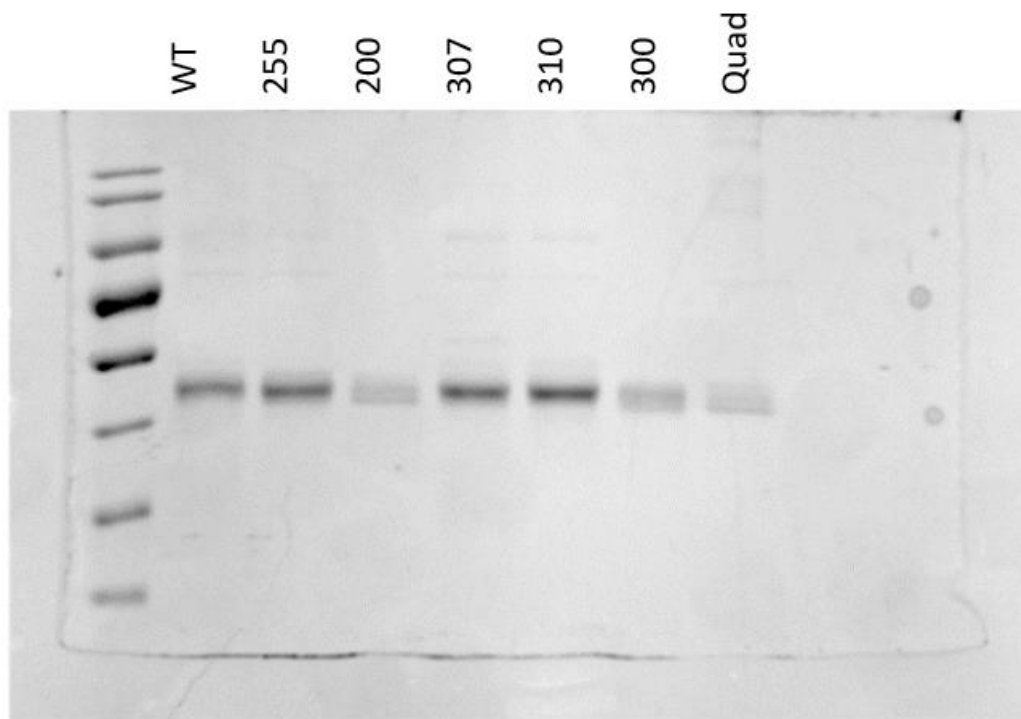


Figure A.3 Purification of CSE mutants.

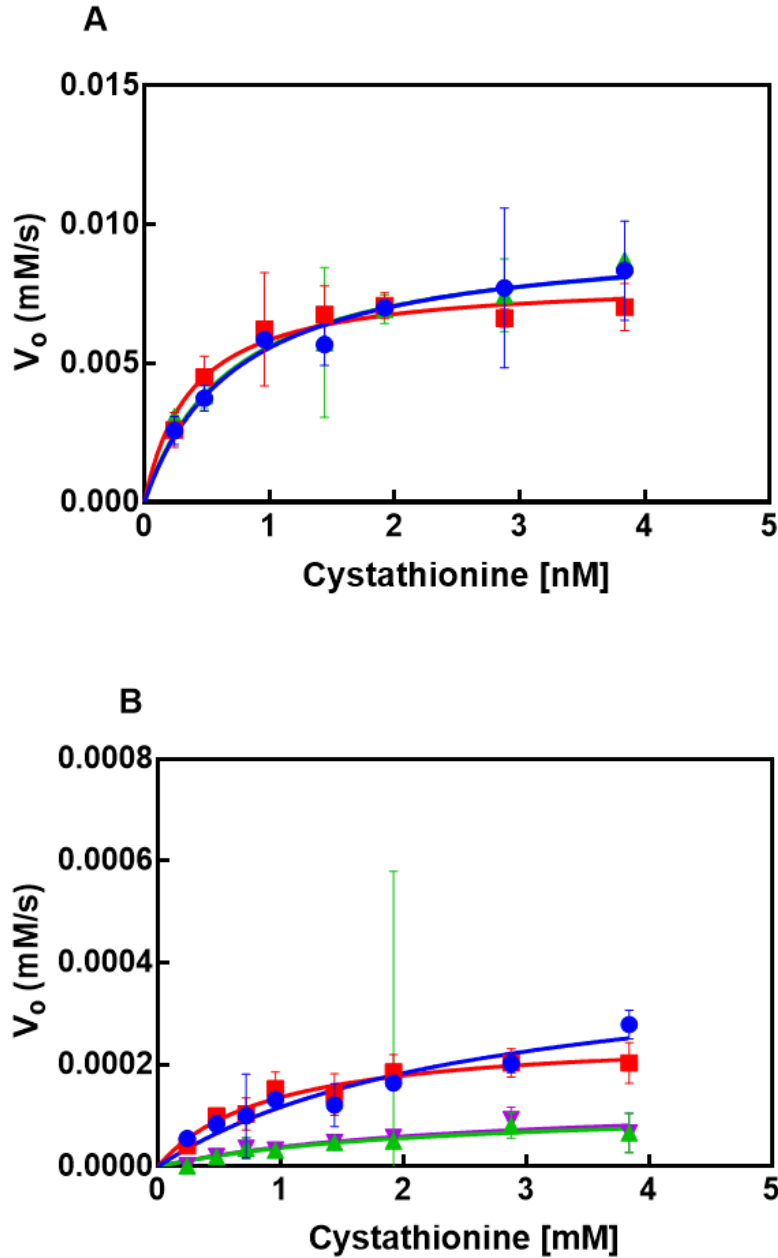


Figure B.1 Effects of post-translational modifications on CSE (A) Reduction and oxidation of CSE *via* GSH and GSSG treatment of CSE. WT, blue; WT + GSH, red; WT + GSSG, green. (B) Incubation of WT and 300-double mutant with GSNO. WT, blue; WT + GSNO, red; 307_310 green, 307_310 + GSNO, purple.

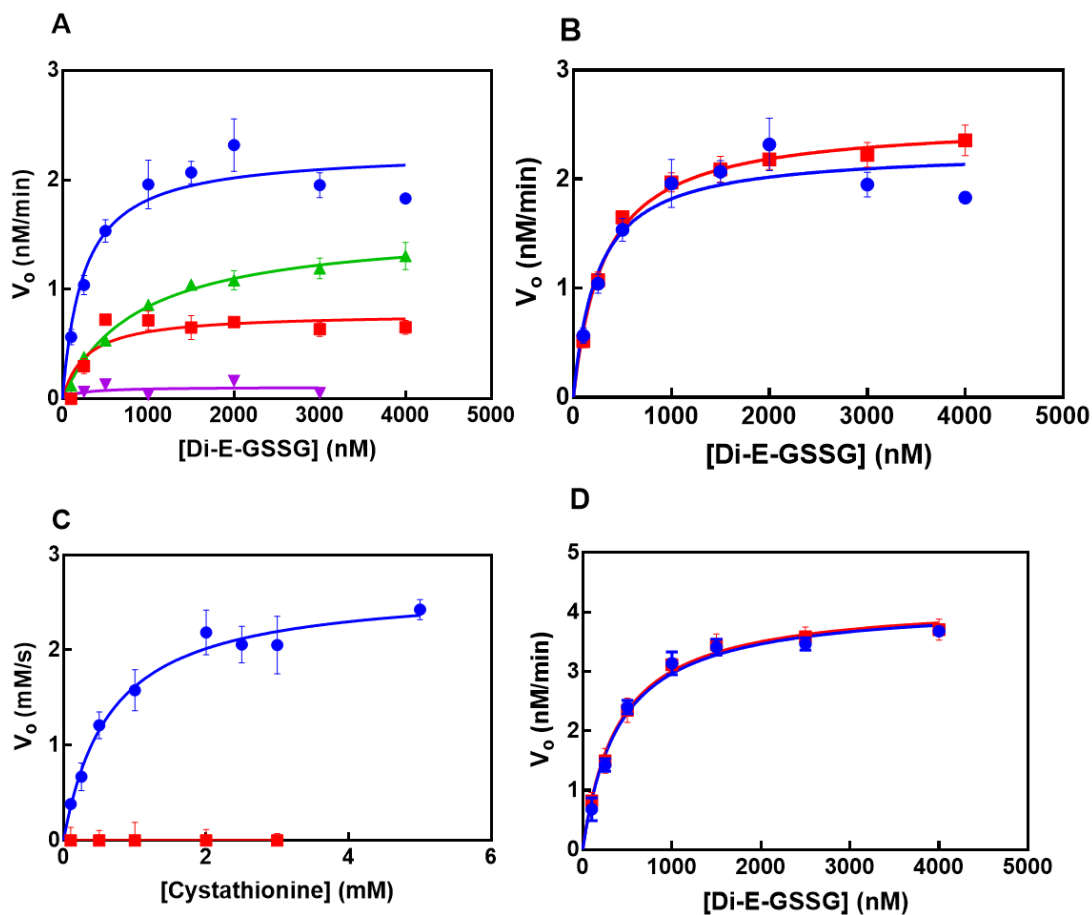


Figure B.2 Reaction of WT, 200, 300, and quad with Di-E-GSSG. (A) (WT; blue, 307_310; green, 252_255; red, quad; purple). (B) Summation of 200 and 300 rates, equaling the WT rate (WT; blue, combined 200 and 300; red). (C) Cystathionine catabolism with inhibited WT by PAG and uninhibited WT (WT; blue, inhibited WT; red). (D) Di-E-GSSG observed rates with inhibited and uninhibited WT.

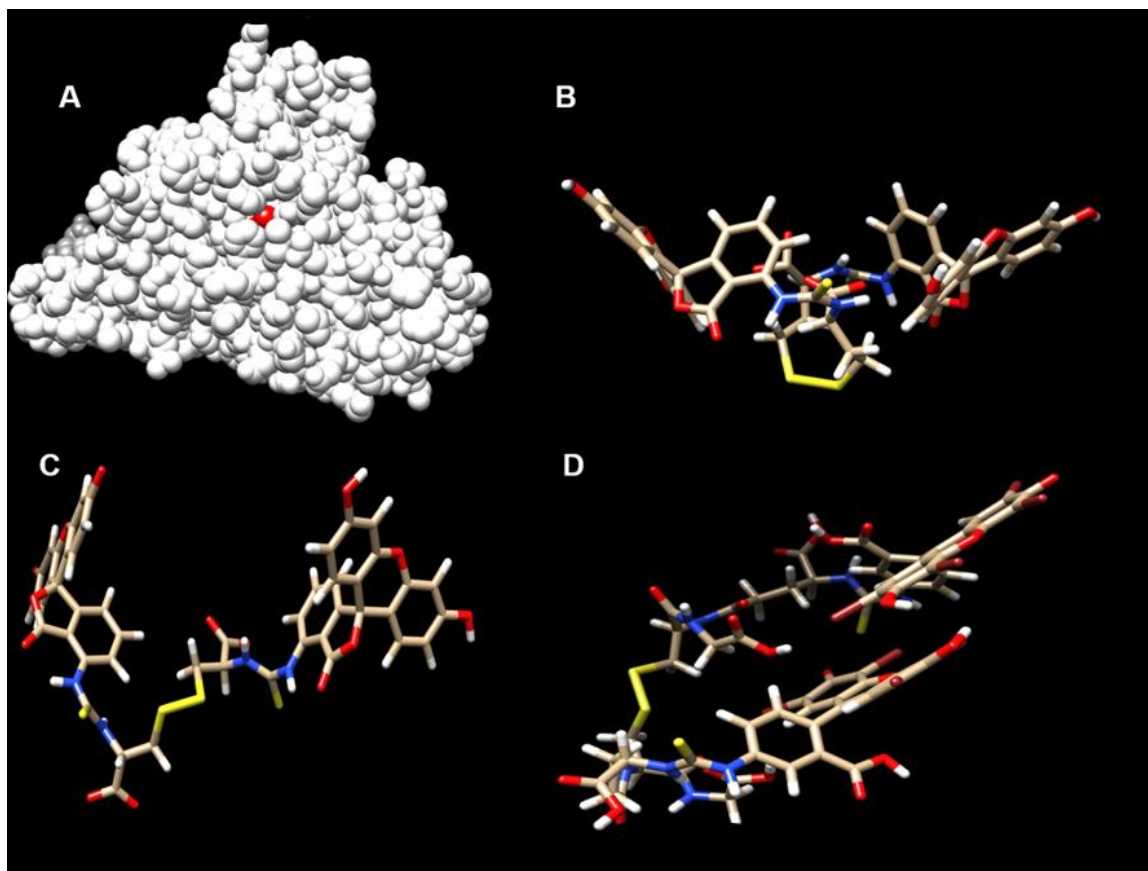


Figure B. 3 (A) Space filling model of CSE crystal structure 2NMP. Cysteine 310 is shown in red and is shown as solvent accessible. This residue is solvent exposed on all 4 monomers. (B) Energy minimized structure of FITC₂-homocystine showing a disulfide-dihedral angle of 62.2 °. (C) Energy minimized structure of FITC₂-cystine showing a disulfide dihedral angle of 89.8 °. (D) Energy minimized structure of FITC₂-GSSG showing a disulfide-dihedral angle of 127.2 °.

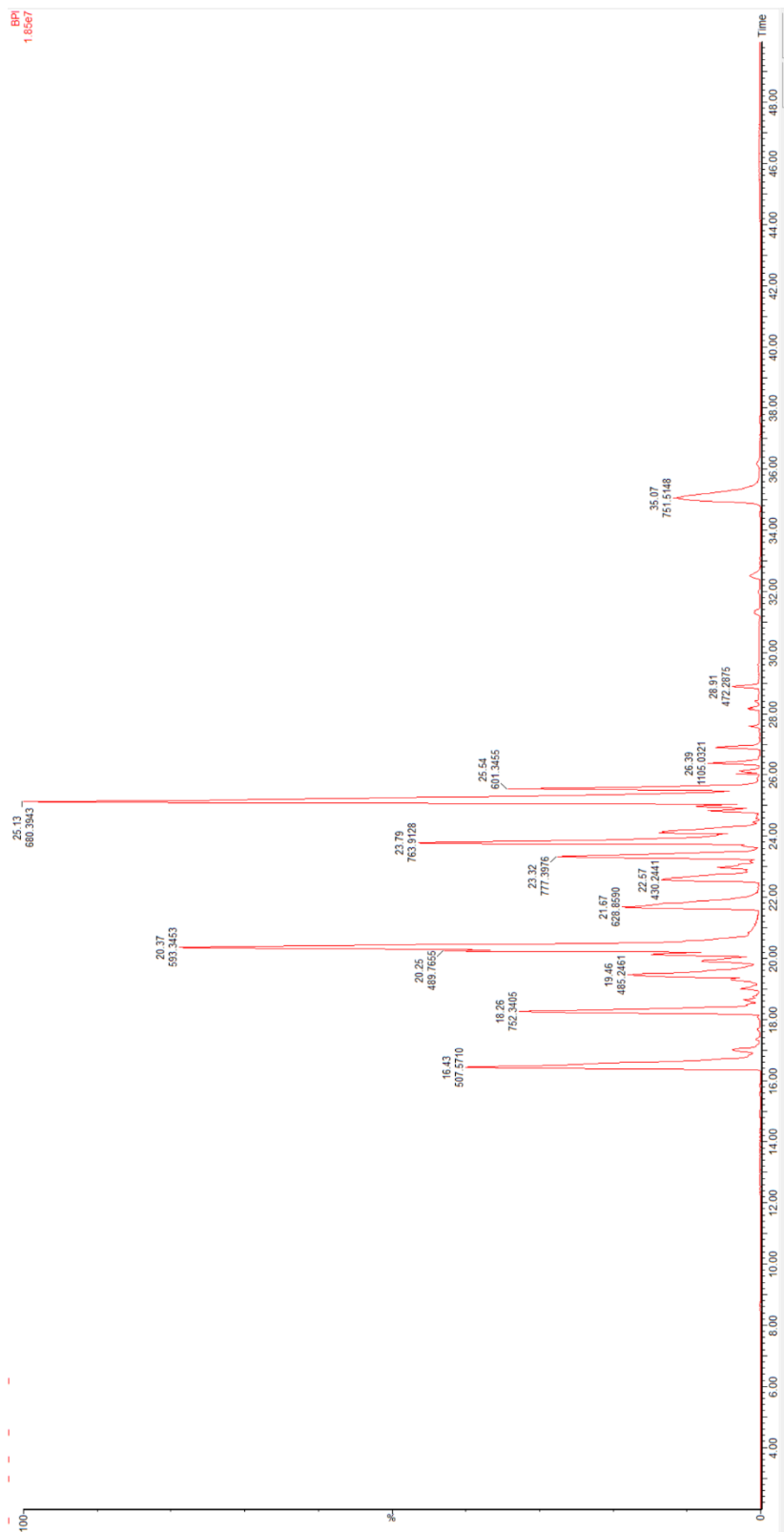


Figure B.4 Supplementary Mass spec data. The chromatogram of *WT* CSE. The 1105 m/z indicates the 200 motif.

TLHVRMEK

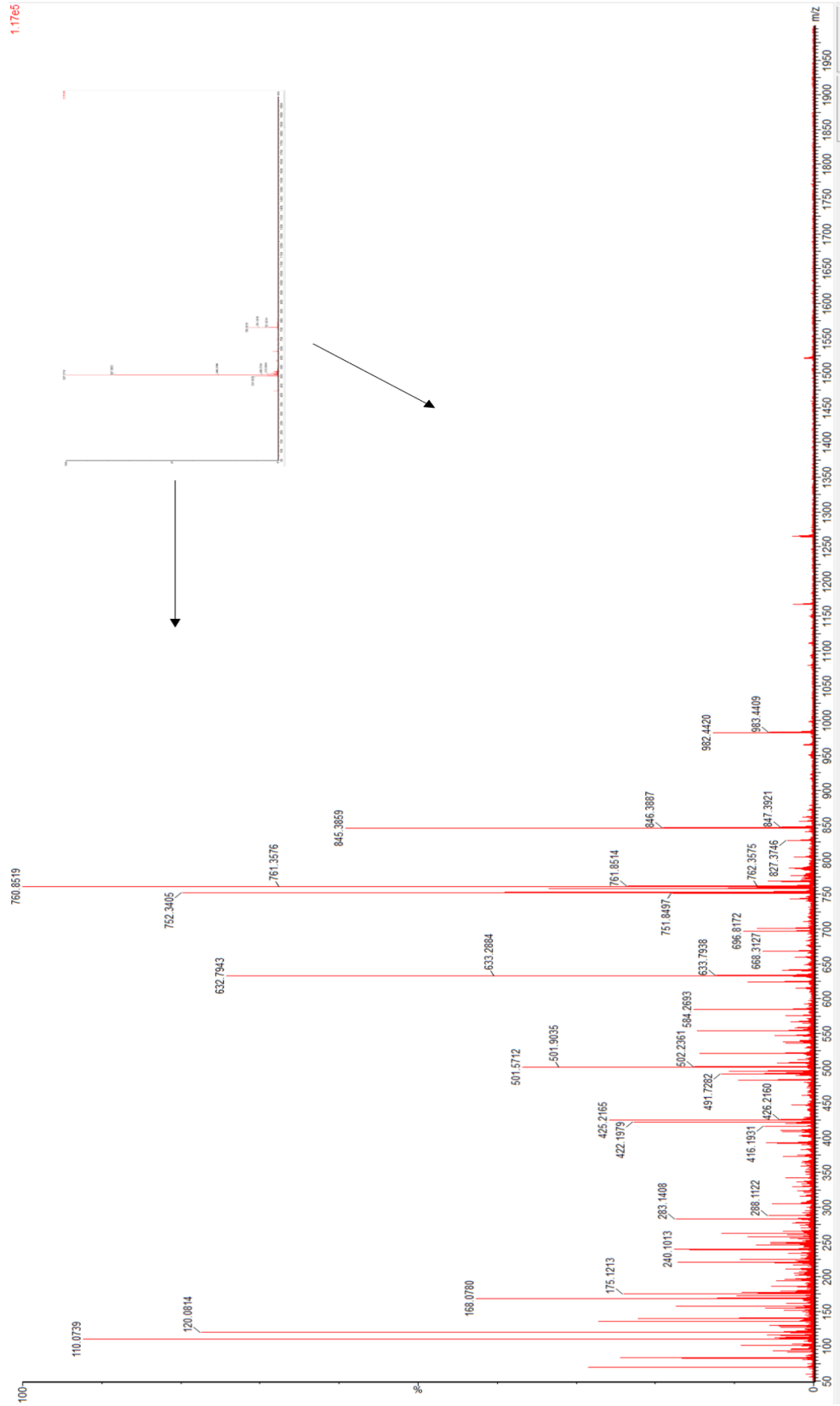


Figure B.5 Identifying peptide for CSE.

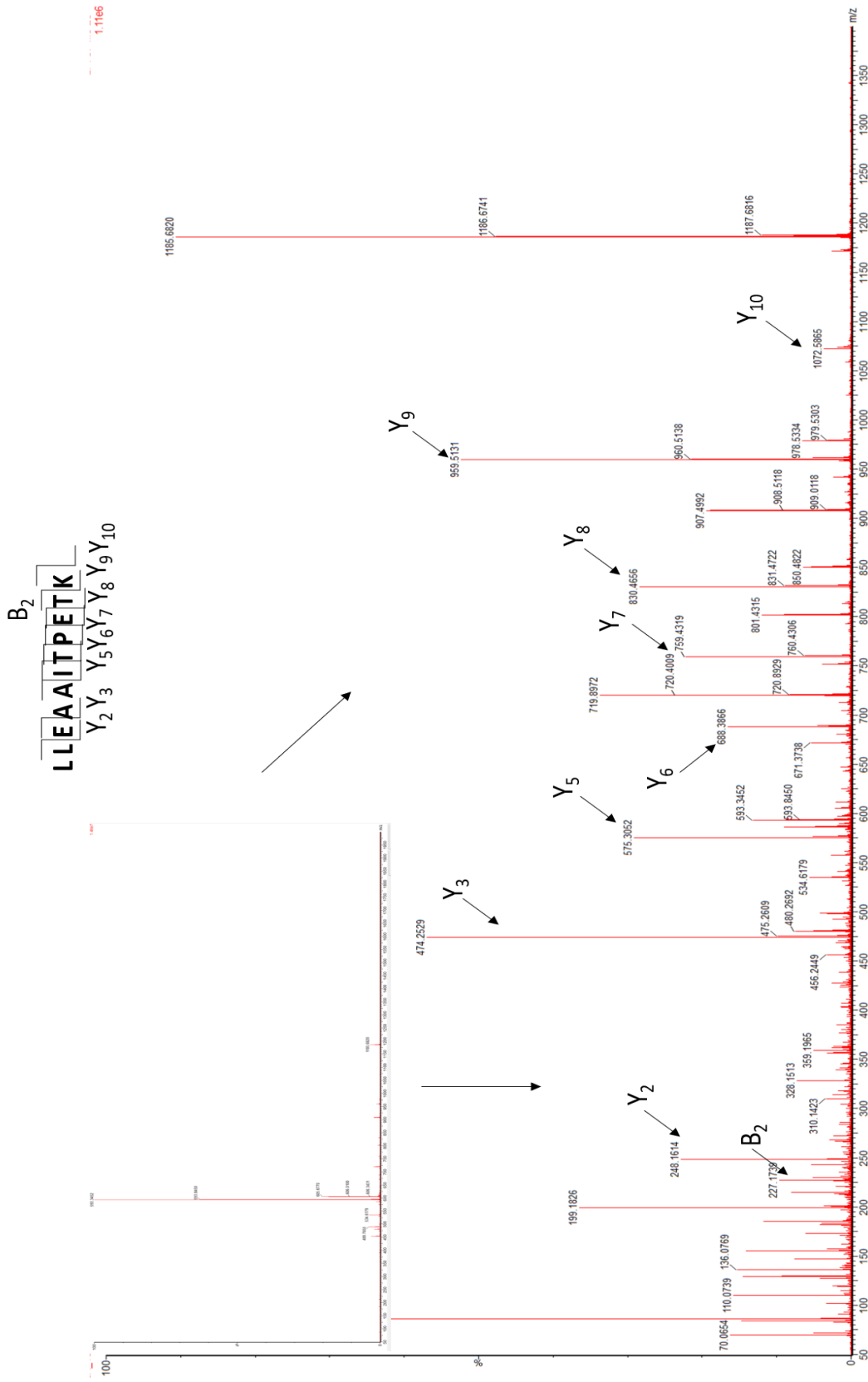


Figure B.6 Identifying peptide for CSE.

VITA AUCTORIS

NAME: Scott Andrew Smith

PLACE OF BIRTH: Windsor, ON

YEAR OF BIRTH: 1991

EDUCATION: Villanova High School, LaSalle, ON, 2009

University of Windsor, B.Sc., Windsor, ON,
2014

University of Windsor, M.Sc., Windsor, ON,
2019